Mathematical Biosciences 325 (2020) 108368

Contents lists available at ScienceDirect

Mathematical Biosciences

journal homepage: www.elsevier.com/locate/mbs

Original research article

Insecticide resistance and malaria control: A genetics-epidemiology modeling approach

Jemal Mohammed-Awel [a,*], Enahoro A. Iboi [b], Abba B. Gumel [b]

[a] Department of Mathematics, Valdosta State University, Valdosta, GA 31698, USA
[b] School of Mathematical and Statistical Sciences, Arizona State University, Tempe, AZ, 85287, USA

ARTICLE INFO

Keywords:
Malaria
Insecticide resistance
Population genetics
Equilibria
Stability
Effective control window

ABSTRACT

Malaria, a deadly infectious disease caused by the protozoan *Plasmodium*, remains a major public health menace affecting at least half the human race. Although the large-scale usage of insecticides-based control measures, notably long-lasting insecticidal nets (LLINs) and indoor residual spraying (IRS), have led to a dramatic reduction of the burden of this global scourge between the period 2000 to 2015, the fact that the malaria vector (adult female *Anopheles* mosquito) has become resistant to all currently-available insecticides potentially makes the current laudable global effort to eradicate malaria by 2040 more challenging. This study presents a novel mathematical model, which couples malaria epidemiology with mosquito population genetics, for assessing the impact of insecticides resistance on malaria epidemiology. Numerical simulations of the model, using data relevant to malaria transmission dynamics in the Jimma Zone of Southwestern Ethiopia, show that the implementation of a control strategy based on using LLINs alone can lead to the effective control of malaria, while also effectively managing insecticide resistance, if the LLINs coverage in the community is high enough (over 90%). It is further shown that combining LLINs with IRS (both at reduced and realistically-attainable coverage levels) can lead to the aforementioned effective control of malaria and effective management of insecticide resistance if their coverage levels lie within a certain *effective control window* in the LLINs-IRS coverage parameter space (this result generally holds regardless of whether or not larviciding is implemented in the community). The study identifies three key parameters of the model that negatively affect the size of the effective control window, namely parameters related with the coverage level of larviciding, the number of new adult mosquitoes that are females and the initial size of the frequency of resistant allele in the community. For the coverage of LLINs and IRS within the effective control window, an additional increase in the values of the aforementioned three parameters may lead to a shrinkage in the size of the effective control window (thereby causing the failure of the insecticides-based control).

1. Introduction

Malaria, caused by the protozoan *Plasmodium* parasites, has historically being one of the deadliest infectious diseases to befall mankind. Since the cross of *Plasmodium falciparum* (the deadliest of the five species of the *Plasmodium* parasites [1,2]) to humans some 10,000 years ago [3], malaria continues to pose major public health challenges in many parts of the world (with over 2.5 billion people at risk) [4]. Malaria caused 228 million infections and 405,000 deaths (with majority of the deaths occurring in children under the age of five) globally in 2018 [4]. The disease is spread between humans following effective bites by malaria-infected adult female *Anopheles* mosquitoes. The adult female mosquito bites humans in search of bloodmeal needed for egg development. If the mosquito is infected, such a bite may lead to the transfer of the *Plasmodium* parasite to the human host (making the human infected). Similarly, if the mosquito is uninfected and the bite is on an infected human, the mosquito can become infected. The *Anopheles* lifecycle consists of the three aquatic stages (namely, eggs stage, larval stage and pupal stage) and an adult stage [5,6].

Owing to the devastating burden of malaria, numerous global efforts have been embarked upon aimed at reducing or eliminating the menace of malaria. One of such efforts was the Roll Back Malaria initiative, which resulted in a dramatic reduction of malaria burden in sub-Saharan Africa between 2000–2015 [7–9]. The success of this initiative was largely believed to be due to the widespread use of insecticides-based mosquito control measures, such as long-lasting insecticidal nets (LLINs) and indoor residual spraying (IRS), although other measures (such as early diagnosis, improved anti-malaria drug therapy and improved public health infrastructure were also a factor) [8]. Five major classes of insecticide are used in malaria control

* Corresponding author.
E-mail address: jmohammedawel@valdosta.edu (J. Mohammed-Awel).

https://doi.org/10.1016/j.mbs.2020.108368
Received 14 January 2020; Received in revised form 19 April 2020; Accepted 29 April 2020
Available online 11 May 2020

efforts, namely *pyrethroids, organochlorines, organophosphates, neonicotinoids* and *carbamates*. Although all five of these agents are used for IRS, only the *pyrethroids* is used in LLINs (this is due to their low mammalian toxicity and high irritant effect on adult mosquitoes) [10]. It was estimated that bednets and IRS jointly account for about 81% of the reduction of malaria burden recorded during the 2000–2015 period (with most of the benefits attributed to the use of the bednets) [11]. These dramatic successes prompted the emergence of other laudable initiatives aimed at eradicating malaria. These include The Global Technical Strategy for Malaria 2016–2030 (approved by the World Health Assembly in May 2015 [9]) and the $ZeroX40$ Initiative (an initiative of five chemical companies with the support of the Bill & Melinda Gates Foundation and the Innovative Vector Control Consortium [12,13]), aimed at eradicating malaria by 2030 or 2040, respectively. These eradication efforts are mostly focused on the use of the aforementioned insecticides-based mosquito control measures.

Unfortunately, the successes recorded in the fight against malaria (for the period 2000 to 2015) are now threatened largely owing to the fact that the heavy use of the insecticides-based control measures resulted in the emergence of *Anopheles* resistance to each of the aforementioned chemical agents used in LLINs and IRS [6,14–21]. As noted by Mohammed-Awel and Gumel [22], mosquitoes (or disease vectors in general) are said to be resistant to insecticides when the insecticides are no longer able to kill them on contact, or when they resist and survive the effect of the insecticides resistance and become able to reproduce in an insecticide-treated environment (or after being in contact with the chemical insecticides). Thus, the emergence and widespread nature of this vector insecticide resistance certainly poses serious threats to the effectiveness of LLINs and IRS. Since LLINs and IRS are the cornerstones of all the current malaria eradication efforts (particularly LLINs), any threat on their effectiveness (due to vector insecticide resistance) is a direct threat to the malaria eradication efforts. Thus, a key modeling objective will be to design insecticides-based strategies (using LLINs and IRS) that effectively combats malaria spread, while also effectively managing insecticide resistance. Unfortunately, however, there is still no clear evidence or consensus of association (if any) between *Anopheles* insecticide resistance and malaria epidemiology [14,23–26]. In fact, while a recent study shows that insecticide resistance could lead to a rebound in malaria [14,27], another recent study (based on a very large observational cohort across five countries in Africa) found no relationship between laboratory-assessed insecticide resistance and malaria epidemiology [24,25].

One reason why the exact effect (if any) vector insecticide resistance would have on malaria epidemiology is unknown is the absence of precise quantification of the fitness costs of insecticide resistance on the resistant vector population (both in the lab and under field conditions). It seems reasonable to assume that such fitness costs, particularly if they manifest in terms of heterogeneities with respect to increase or decrease in adult mosquito survival, biting, mating success, host-seeking and delayed mortality [24,28], could significantly affect malaria epidemiology [24]. Sexual heterogeneity in the adult mosquito is another important aspect to consider, since the lifecycles of the adult male and female *Anopheles* mosquitoes vary markedly (for instance, only the adult female mosquitoes seek bloodmeals from humans). Thus, the balance of fitness costs and benefits of insecticide resistance may vary appreciably between the sexes, with implications for both the spread of insecticide resistance alleles and malaria epidemiology [24]. The aforementioned uncertainties (of the precise relationship, if any, between insecticide resistance and malaria epidemiology) notwithstanding, the absence of new viable alternatives to the existing insecticides (and considering the generally long duration before any new and potent insecticides are available in the markets), it is of great public health interest to determine how best to use the existing (*albeit* limited) insecticides-based resources to combat malaria while also effectively managing *Anopheles* resistance to those chemical resources.

The study of the population genetics of the malaria vector is also critical to the problem of quantifying the relationship between insecticide resistance and malaria epidemiology. In the context of the study of insecticide resistance and malaria dynamics, the study of the population genetics of the mosquito entails the characterization of the genetic variation within, and among, the mosquito populations (and the evolutionary factors that explain this variation) [22,29]. In particular, the study of the population genetics of the malaria vector allows for the quantification of the frequencies (and spread) of the insecticide resistant alleles and genotypes in the mosquito populations [15,22,29–31]. Physiological mechanisms within the mosquito that decrease the insecticide toxicity often arise due to changes in one or several genes of the mosquito [32], and mosquitoes that express the distinct genetic makeup pass along the genes for resistance to the next generation. In other words, insecticide resistance can be inherited and passed from one generation to the next [22,29,32]. Gradually, the frequency of the allele that determines resistance, as well as the proportion of resistant mosquitoes in the community, increases over time (and, through this process of selection, the mosquito population in the community gradually develops resistance to the insecticides [22,29,33]).

Mathematical models that incorporate the population genetics of the malaria vector have been developed and used to study the community-level impact of insecticide resistance on the population ecology of the malaria vector [15,16,22,29–31,34–36]. These models were typically of the form of deterministic systems of nonlinear differential or difference equations. Levick et al. [35] presented a two-locus deterministic difference equation model for the spread of insecticide resistance in mosquito populations. By using the model to investigate the relative merits of the sequential use of insecticides versus their mixture, their study showed that mixtures are favored when the effectiveness of the insecticides is high and if vector exposure to the insecticides (i.e., if the proportion of mosquitoes that encounter the insecticide) is low. Moreover, if the insecticides are not effective in killing homozygous sensitive adult mosquitoes, then the sequential deployment of the insecticides is the more effective strategy in controlling the targeted mosquito population (it should be mentioned that the model in [35] does not include equations for the dynamics of malaria disease in humans or mosquitoes).

Barbosa et al. [16] presented a deterministic difference equation model that incorporate the immature mosquito dynamics, adult mosquito sex structure, mosquito population genetics and malaria epidemiology. Their study showed that linking vector immature and sex-structure with mosquito population genetics (*vis a vis* vector insecticide resistance) play a key role in designing sustainable control strategies. The model in the Barbosa et al. study [16] does not include equations for the dynamics of malaria disease in humans or mosquitoes. Mohammed-Awel and Gumel [22] developed a differential equation model for malaria transmission dynamics, which combined mosquito population genetics (for insecticide resistance in mosquitoes) and malaria dynamics in a population. Their study [22] emphasized the important role parameters related to the level of insecticide resistant allele dominance (in mosquitoes with heterozygous genotype) and numerous fitness costs of the insecticide resistance in the vector population. The model in [22] does not incorporate the dynamics of aquatic (immature) mosquitoes, male mosquitoes, and larvicides-based vector control.

It should be mentioned that, while many of the aforementioned modeling studies have considered the population genetics of the malaria vector harboring resistance to the chemical insecticides in LLINs and IRS (i.e., the models considered the distribution of insecticide resistant alleles in the community) [15,16,22,29–31,34–36], very few of these models actually combine this (i.e., mosquito population genetics) with the population-level dynamics of malaria (i.e., malaria epidemiology in both the human host and in the mosquito). In fact, to the authors' knowledge, there is no mathematical model to-date that incorporates the details of the complex *Anopheles* lifecycle, genotype structure in mosquito for the gene that confers insecticide resistance, and the disease dynamics in humans and mosquitoes [22,29,36].

The purpose of the current study is to extend the aforementioned modeling studies (that incorporate the population genetics of the malaria vector) by designing a novel model that, additionally, allows for the assessment of other pertinent aspects of malaria epidemiology and the population ecology and genetics of the malaria mosquito. In particular, the new model to be developed will incorporate the detailed genotype structure of the gene that confers insecticide resistance in mosquitoes. Doing this allows for the realistic investigation of malaria transmission dynamics (in humans and mosquitoes) and the evolution (spread) of insecticide resistance in the mosquito population simultaneously. Some of the other specific extensions in the new model to be developed include the dynamics of aquatic (immature) malaria mosquitoes (thereby allowing for the realistic assessment of larvicide-based control measures), the dynamics of both male and female *Anopheles* mosquitoes (thereby allowing for the realistic accounting of the mating processes, as well as the assessment of the impact of altering the sex-ratio in the disease transmission and the evolution of insecticide resistance), and numerous pertinent fitness costs associated with insecticide resistance. Furthermore, a novel nonlinear genotype-specific mosquito biting rate function will be developed and used to study the dynamics of the model. The model to be developed allows for the assessment of all three insecticides-based interventions, namely the use of larvicides, LLINs and IRS.

The paper is organized as follows. The model is formulated in Section 2. Rigorous results for the existence and asymptotic stability of the various disease-free equilibria of the model are given in Section 3. Numerical simulations of the model, using data relevant to malaria transmission dynamics in Jimma zone of Ethiopia (an area of high malaria transmission), are reported in Section 4.

2. Formulation of mathematical model

2.1. State variables and basic definitions

SEIR model for the human population and a model for mosquito population dynamics with detailed mosquito life-cycle (aquatic (egg, larvae, and pupae) and adult) with genotype-structure (for insecticide resistance) and sex structure (at adult stage) is presented. The total human population is stratified according to their LLINs and/or IRS usage (we adopt the notation that humans/homes that use LLINs and/or IRS are categorized as "protected", while those that do not are "unprotected"). The human population is classified as susceptible protected (unprotected) $S_{H_p}(t)$ ($S_{H_u}(t)$), exposed protected (unprotected) $E_{H_p}(t)$ ($E_{H_u}(t)$), infectious protected (unprotected) $I_{H_p}(t)$ ($I_{H_u}(t)$), and recovered protected (unprotected) $R_{H_p}(t)$ ($R_{H_u}(t)$) humans. Thus, the total human population at time t is given by:

$$N_H(t) = S_{H_p}(t)+S_{H_u}(t)+E_{H_p}(t)+E_{H_u}(t)+I_{H_p}(t)+I_{H_u}(t)+R_{H_p}(t)+R_{H_u}(t).$$

As discussed in the above section, mosquito insecticide resistance is determined by a single gene of two alleles (resistant (R) and susceptible (S) alleles). Indoor-residual spray (IRS) and larvicides are included for mosquito. The total mosquito population at time t is split into mutually-exclusive compartments of homozygous sensitive eggs ($E_{SS}(t)$), heterozygous eggs ($E_{RS}(t)$), homozygous resistant eggs ($E_{RR}(t)$), homozygous sensitive larvae ($L_{SS}(t)$), heterozygous larvae ($L_{RS}(t)$), homozygous resistant larvae ($L_{RR}(t)$), homozygous sensitive pupae ($P_{SS}(t)$), heterozygous pupae ($P_{RS}(t)$), homozygous resistant pupae ($P_{RR}(t)$), homozygous sensitive adult female mosquitoes (Susceptible ($S^f_{SS}(t)$), Exposed ($E^f_{SS}(t)$), and Infected ($I^f_{SS}(t)$)), heterozygous adult female mosquitoes (Susceptible ($S^f_{RS}(t)$), Exposed ($E^f_{RS}(t)$), and Infected ($I^f_{RS}(t)$)), homozygous resistant adult female mosquitoes (Susceptible ($S^f_{RR}(t)$), Exposed ($E^f_{RR}(t)$), and Infected ($I^f_{RR}(t)$)), homozygous sensitive adult male mosquitoes ($M^m_{SS}(t)$), heterozygous adult male mosquitoes ($M^m_{RS}(t)$), and homozygous resistant adult male mosquitoes ($M^m_{RR}(t)$). Thus, the total eggs ($E(t)$), the total larvae ($L(t)$), the total pupae ($P(t)$) the total adult female population ($M^f(t)$), the total adult male population ($M^m(t)$), and the total mosquito population ($M(t)$) are

$$\begin{aligned}
E(t) &= E_{SS}(t)+E_{RS}(t)+E_{RR}(t),\\
L(t) &= L_{SS}(t)+L_{RS}(t)+L_{RR}(t),\\
P(t) &= P_{SS}(t)+P_{RS}(t)+P_{RR}(t),\\
M(t) &= M^f(t)+M^m(t),\\
M^f(t) &= M^f_{SS}(t)+M^f_{RS}(t)+M^f_{RR}(t),\\
M^m(t) &= M^m_{SS}(t)+M^m_{RS}(t)+M^m_{RR}(t),\\
M^f_{SS}(t) &= S^f_{SS}(t)+E^f_{SS}(t)+I^f_{SS}(t),\\
M^f_{RS}(t) &= S^f_{RS}(t)+E^f_{RS}(t)+I^f_{RS}(t),\\
M^f_{RR}(t) &= S^f_{RR}(t)+E^f_{RR}(t)+I^f_{RR}(t).
\end{aligned} \tag{2.1}$$

For communities where LLINs are used, the genotypic-specific average biting rate (i.e., the average number of bites *per* mosquito of i-genotype *per* unit time), denoted by b_i (with i representing the genotype SS, RS or RR), can be defined by the following nonlinear function:

$$b_{SS} = \frac{(1-\varepsilon_B^{SS}C_B)b_{max}}{1+\varepsilon_B^{SS}C_B b_{max}},\quad b_{RS} = \frac{(1-\varepsilon_B^{RS}C_B)b_{max}}{1+\varepsilon_B^{RS}C_B b_{max}},\quad \text{and}$$
$$b_{RR} = \frac{(1-\varepsilon_B^{RR}C_B)b_{max}}{1+\varepsilon_B^{RR}C_B b_{max}}, \tag{2.2}$$

where, $0 \le C_B \le 1$ is the proportion of individuals in the community who use LLINs (i.e., proportion of individuals in the community who are protected from mosquito bites by LLINs), $0 \le \varepsilon_B^i \le 1$, with $i = SS, RS, RR$ is the efficacy of the bednet (LLIN) to protect humans from bites by adult female mosquitoes of i-genotype and b_{max} is maximum mosquito biting rate. The proposed nonlinear genotype-specific biting rate function (2.2) is novel, and it is instructive to show that it captures all the pertinent properties of a realistic mosquito biting rate function. This is done below, by considering the three possible cases for the LLINs coverage (C_B) and genotype-specific efficacy (ε_B^i) pairs:

(i) LLINs coverage and efficacy at 100% each (i.e., $C_B = 1$ and $\varepsilon_B^i = 1$ for $i = SS, RS, RR$): In this case, it follows from (2.2) the genotype-specific average biting rate (b_i) reduces to zero (i.e., $b_i = 0$). That is, mosquitoes are unable to bite humans if LLINs efficacy is 100% and every member of the community sleeps under such net (i.e., $C_B = 1$).

(ii) LLINs coverage and efficacy at 0% each (i.e., $C_B = \varepsilon_B^i = 0$ with $i = SS, RS, RR$): For this case, the average genotype-specific biting rate (b_i) attains its maximum value (i.e., $b_i = b_{max}$). That is, mosquitoes enjoy maximum biting rate when humans are not sleeping under any net (i.e., all humans are unprotected).

(iii) LLINs coverage and efficacy in the ranges $0 < C_B < 1$ and $0 < \varepsilon_B^i < 1$ for $i = SS, RS, RR$: In this case (where LLINs coverage and efficacy are not 100% or 0% effective), sensitivity analysis can be carried out on the biting rate function (2.2) to determine if it behaves in the way expected. In particular, it can be seen from (2.2) that the elasticity indices associated with the biting rate for mosquitoes of SS genotype (b_{SS}), with respect to the LLINs coverage (C_B) and efficacy (ε_B^{SS}), are given, respectively, by:

$$\frac{\varepsilon_B^{SS}}{b_{SS}}\frac{\partial b_{SS}}{\partial \varepsilon_B^{SS}} = \frac{-\varepsilon_B^{SS}C_B\left[(1+\varepsilon_B^{SS}C_B b_{max})+b_{max}(1-\varepsilon_B^{SS}C_B)\right]}{(1-\varepsilon_B^{SS}C_B)(1+\varepsilon_B^{SS}C_B b_{max})} < 0,$$
since $0 < \varepsilon_B^{SS}\ C_B < 1$,

and,

$$\frac{C_B}{b_{SS}}\frac{\partial b_{SS}}{\partial C_B} = \frac{-\varepsilon_B^{SS}C_B\left[(1+\varepsilon_B^{SS}C_B b_{max})+b_{max}(1-\varepsilon_B^{SS}C_B)\right]}{(1-\varepsilon_B^{SS}C_B)(1+\varepsilon_B^{SS}C_B b_{max})} < 0,$$
since $0 < \varepsilon_B^{SS}\ C_B < 1$.

It follows from the above inequalities that increasing the coverage (C_B) and efficacy (ε_B^{SS}) of LLINs decreases the average biting rate

b_{SS} (as expected). The same results can be established by computing the sensitivity indices associated with the biting rate of mosquitoes of RS and RR genotypes. Thus, the novel genotype-specific biting rate function (2.2) captures all the pertinent properties of a suitable biting rate function for mosquitoes. Hence, it is suitable for use in a realistic modeling study for the dynamics of mosquito-borne diseases, such as malaria.

The infection rates (*forces of infections*) for malaria transmission are defined by:

$$\lambda_{HV}^{i^{SS}} = \frac{\beta_V b_{SS} I_{H_p}}{N_H}, \quad \lambda_{HV}^{i^{RS}} = \frac{\beta_V b_{RS} I_{H_p}}{N_H} \quad \lambda_{HV}^{i^{RR}} = \frac{\beta_V b_{RR} I_{H_p}}{N_H},$$
$$\lambda_{HV}^{u} = \frac{\beta_V b_{max} I_{H_u}}{N_H},$$
$$\lambda_{VH}^{i^{SS}} = \frac{\beta_H b_{SS} I_{SS}^f}{N_H}, \quad \lambda_{VH}^{i^{RS}} = \frac{\beta_H b_{RS} I_{RS}^f}{N_H}, \quad \lambda_{VH}^{i^{RR}} = \frac{\beta_H b_{RR} I_{RR}^f}{N_H} \text{ and}$$
$$\lambda_{VH}^{u} = \frac{\beta_H b_{max} (I_{SS}^f + I_{RS}^f + I_{RR}^f)}{N_H}, \tag{2.3}$$

where $\lambda_{HV}^{i^j}$ represents the transmission rate from infectious protected humans to susceptible mosquitoes (of i-genotype), $\lambda_{VH}^{i^j}$ represents the rate at which infectious mosquitoes (of i-genotype) transmit infection to protected susceptible humans (where $i = SS,\ RS,\ RR$). Similarly, λ_{VH}^{u} represents the rate at which infectious mosquitoes transmit malaria to unprotected susceptible humans, while β_H (β_V) represents the probability of disease transmission from infectious mosquitoes (humans) to susceptible humans (mosquitoes).

In the formulation of the novel mathematical model to be developed in this study, it is assumed that mating in the adult mosquito population (between opposite sexes) is random [29]. That is, all adult mosquitoes have the same chance of reproducing, and they mate with any other adult mosquito (of opposite sex) in the population with the same probability. The frequency of each allele (i.e., sensitive (S) or resistant (R) allele) for adult male and female mosquitoes is calculated using the following formulas [29,30,37]:

$$q_f(t) = \frac{M_{SS}^f(t) + \frac{1}{2}M_{RS}^f(t)}{M^f(t)}, \quad p_f(t) = \frac{M_{RR}^f(t) + \frac{1}{2}M_{RS}^f(t)}{M^f(t)},$$
$$q_m(t) = \frac{M_{SS}^m(t) + \frac{1}{2}M_{RS}^m(t)}{M^m(t)}, \quad p_m(t) = \frac{M_{RR}^m(t) + \frac{1}{2}M_{RS}^m(t)}{M^m(t)}, \tag{2.4}$$

where $q_f(t)$ ($q_m(t)$) represents the frequency of sensitive allele (S) in female (male) adult mosquitoes, and $p_f(t)$ ($p_m(t)$) represents the frequency of resistant allele (R) in female (male) adult mosquitoes. Mosquito resistance is determined by a single gene of two alleles. For example, for the adult female mosquito population, there are two S alleles (S copies) in each gene of an SS-genotype mosquito, one copy of the S allele in each gene of RS-genotype mosquito and no copy of S allele in the gene of an RR-genotype mosquito. Therefore, the proportion of S alleles in the female population is $q_f(t) = \frac{2M_{SS}^f(t) + M_{RS}^f(t)}{2M^f(t)} = \frac{M_{SS}^f(t) + \frac{1}{2}M_{RS}^f(t)}{M^f(t)}$. Thus, the probability that the mating between an adult female and an adult male mosquito will lead to the formation of eggs of SS-genotype is $q_f(t) \times q_m(t)$. Similarly, the probability that such mating produces eggs of RS-genotype is $p_f(t) \times q_m(t) + p_m(t) \times q_f(t)$ (that is, $p_f(t) \times q_m(t)$ accounts for an R allele from the female and as S allele from the male partner) plus $p_m(t) \times q_f(t)$ (which accounts for an R allele from the male and an S allele from the female). Finally, the probability that such mating produces eggs of RR-genotype is $p_f(t) \times p_m(t)$. Consequently, the proportion of mosquitoes in the community with the SS, RS and RR genotype in the next generation (i.e., at time $t + \Delta t$, where $\Delta t > 0$ is an increment in time) is given by the quantities $q_f(t)q_m(t)$, $p_f(t)q_m(t) + p_m(t)q_f(t)$ and $p_f(t)p_m(t)$, respectively [29]. It should be observed that $q_f(t) + p_f(t) = 1$, $q_m(t) + p_m(t) = 1$ and $q_f(t)p_f(t) + (p_f(t)q_m(t) + p_m(t)q_f(t)) + q_m(t)p_m(t) = 1$ for all time $t \geq 0$ (which is the Hardy–Weinberg condition in population genetics [29,37]).

2.2. Equations of the model

The genetics-epidemiology malaria transmission model to be designed in this study consists of a deterministic system of nonlinear differential equations accounting for the population ecology of the mosquito (both immature and adult) and malaria epidemiology in humans. The equations for the specific life stages of the mosquitoes (both immature and adult) and for the malaria dynamics in the human host are derived as follows.

2.2.1. Immature mosquitoes

The differential equations for the aquatic life stages of immature mosquitoes (eggs, larval and pupal stages) are given by:

Egg stage:

$$\frac{dE_{SS}}{dt} = \psi q_f q_m \left(1 - \frac{E(t)}{K_E}\right)_+ M^f - (\sigma_E^{SS} + \mu_E^{SS})E_{SS},$$
$$\frac{dE_{RS}}{dt} = \psi \left(q_f p_m + q_m p_f\right) \left(1 - \frac{E(t)}{K_E}\right)_+ M^f - (\sigma_E^{RS} + \mu_E^{RS})E_{RS}, \tag{2.5}$$
$$\frac{dE_{RR}}{dt} = \psi p_f p_m \left(1 - \frac{E(t)}{K_E}\right)_+ M^f - (\sigma_E^{RR} + \mu_E^{RR})E_{RR}.$$

Larval stage:

$$\frac{dL_{SS}}{dt} = \sigma_E^{SS} E_{SS} - (\sigma_L^{SS} + \mu_L^{SS} + \varepsilon_L C_L \delta_L)L_{SS},$$
$$\frac{dL_{RS}}{dt} = \sigma_E^{RS} E_{RS} - [\sigma_L^{RS} + \mu_L^{RS} + \varepsilon_L C_L (1 - hu)\delta_L]L_{RS}, \tag{2.6}$$
$$\frac{dL_{RR}}{dt} = \sigma_E^{RR} E_{RR} - [\sigma_L^{RR} + \mu_L^{RR} + \varepsilon_L C_L (1 - u)\delta_L]L_{RR}.$$

Pupal stage:

$$\frac{dP_{SS}}{dt} = \sigma_L^{SS} L_{SS} - (\sigma_P^{SS} + \mu_P^{SS} + \varepsilon_L C_L \delta_P)P_{SS},$$
$$\frac{dP_{RS}}{dt} = \sigma_L^{RS} L_{RS} - [\sigma_P^{RS} + \mu_P^{RS} + \varepsilon_L C_L (1 - hu)\delta_P]P_{RS}, \tag{2.7}$$
$$\frac{dP_{RR}}{dt} = \sigma_L^{RR} L_{RR} - [\sigma_P^{RR} + \mu_P^{RR} + \varepsilon_L C_L (1 - u)\delta_P]P_{RR}.$$

In {(2.5), (2.6), (2.7)}, the parameter ψ is the rate at which eggs are laid by adult female mosquitoes and the quantities q_f and q_m are the allele frequencies defined in (2.4). The environmental carrying capacity of eggs is denoted by K_E, and the notation $(r)_+ = \max\{0, r\}$ is used in the first term of each of the equations in (2.6) to ensure the non-negativity of the logistic egg oviposition term. The parameter μ_j^i ($j = E, L, P$, and $i = SS,\ RS,\ RR$) is the natural death rate of mosquito (of specific genotype). Similarly, σ_j^i ($j = E, L, P$ and $i = SS,\ RS,\ RR$) is the development rate (or hatching rate if $j = E$) of mosquitoes (at life-cycle stage j of genotype i). The parameters δ_L and δ_P represent the maximum insecticides-induced mortality rate for larvae and pupae, respectively (i.e., δ_L and δ_P measure the maximum effectiveness of larvicides to kill immature mosquitoes at the larval and pupal stages). Furthermore, C_L (with $0 \leq C_L \leq 1$ and ε_L represent the coverage and efficacy of larvicides, respectively). Similarly, u (with $0 \leq u \leq 1$) is a modification parameter accounting for the assumed decrease in the mortality rate of the RR-genotype mosquitoes (larvae) due to the use of insecticides (and larvicides), in comparison to the insecticides-induced death rate of adult mosquitoes of SS-genotype. Further, h ($0 \leq h \leq 1$) is a modification parameter accounting for the measure of the dominance of the resistant allele over the sensitive allele (i.e., $h = 1$ models the case where the resistant allele is dominant, and $h = 0$ represents the case when it is recessive). Hence, the quantity $1 - hu$ is a measure of the reduction of the efficacy of insecticides to kill immature mosquitoes with resistant alleles.

2.2.2. Adult mosquitoes

The differential equations for the dynamics of adult (both male and female) mosquitoes are given by:

Adult male mosquitoes:

$$\begin{aligned}
\frac{dM^m_{SS}}{dt} &= (1-r)\sigma_P^{SS}P_{SS} - (\mu_m^{SS} + \varepsilon_A C_A \delta_A)M^m_{SS},\\
\frac{dM^m_{RS}}{dt} &= (1-r)\sigma_P^{RS}P_{RS} - [\mu_m^{RS} + \varepsilon_A C_A(1-hu)\delta_A]M^m_{RS},\\
\frac{dM^m_{RR}}{dt} &= (1-r)\sigma_P^{RR}P_{RR} - [\mu_m^{RR} + \varepsilon_A C_A(1-u)\delta_A]M^m_{RR}.
\end{aligned} \tag{2.8}$$

Adult female mosquitoes:

$$\begin{aligned}
\frac{dS^f_{SS}}{dt} &= r\sigma_P^{SS}P_{SS} - (\lambda_{HV}^{p^{SS}} + \lambda_{HV}^{u})S^f_{SS} - (\mu_f^{SS} + \varepsilon_A(C_B + C_A)\delta_A)S^f_{SS},\\
\frac{dE^f_{SS}}{dt} &= (\lambda_{HV}^{p^{SS}} + \lambda_{HV}^{u})S^f_{SS} - (\theta_{SS} + \mu_f^{SS} + \varepsilon_A(C_B + C_A)\delta_A)E^f_{SS},\\
\frac{dI^f_{SS}}{dt} &= \theta_{SS}E^f_{SS} - (\mu_f^{SS} + \varepsilon_A(C_B + C_A)\delta_A)I^f_{SS},\\
\frac{dS^f_{RS}}{dt} &= r\sigma_P^{RS}P_{RS} - (\lambda_{HV}^{p^{RS}} + \lambda_{HV}^{u})S^f_{RS}\\
&\quad - [\mu_f^{RS} + \varepsilon_A(C_B + C_A)(1-hu)\delta_A]S^f_{RS},\\
\frac{dE^f_{RS}}{dt} &= (\lambda_{HV}^{p^{RS}} + \lambda_{HV}^{u})S^f_{RS} - [\theta_{RS} + \mu_f^{RS} + \varepsilon_A(C_B + C_A)(1-hu)\delta_A]E^f_{RS},
\end{aligned} \tag{2.9}$$

$$\begin{aligned}
\frac{dI^f_{RS}}{dt} &= \theta_{RS}E^f_{RS} - [\mu_f^{RS} + \varepsilon_A(C_B + C_A)(1-hu)\delta_A]I^f_{RS},\\
\frac{dS^f_{RR}}{dt} &= r\sigma_P^{RR}P_{RR} - (\lambda_{HV}^{p^{RR}} + \lambda_{HV}^{u})S^f_{RR}\\
&\quad - [\mu_f^{RR} + \varepsilon_A(C_B + C_A)(1-u)\delta_A]S^f_{RR},\\
\frac{dE^f_{RR}}{dt} &= (\lambda_{HV}^{p^{RR}} + \lambda_{HV}^{u})S^f_{RR} - [\theta_{RR} + \mu_f^{RR} + \varepsilon_A(C_B + C_A)(1-u)\delta_A]E^f_{RR},\\
\frac{dI^f_{RR}}{dt} &= \theta_{RR}E^f_{RS} - [\mu_f^{RR} + \varepsilon_A(C_B + C_A)(1-u)\delta_A]I^f_{RR}.
\end{aligned}$$

In {(2.8), (2.9)}, the parameter r represents the proportion of new adult mosquitoes that are females and λ_{HV}^{u} is the rate of malaria transmission from an unprotected infected human host to a susceptible adult female mosquito (of i genotypes). Similarly, $\lambda_{HV}^{p^i}$ is the rate of malaria transmission from a protected infected human host to a susceptible adult female mosquito (of i genotype). The parameter δ_A is the death rate of adult mosquitoes due to the use of insecticides (i.e., δ_A measure the effectiveness of adulticiding in killing adult mosquitoes of all genotypes). The parameters C_A (with $0 \le C_A \le 1$) and ε_A (with $0 \le \varepsilon_A \le 1$) represent the coverage and efficacy of adulticides (to kill adult mosquitoes) in the community. Natural death rate of adult male (female) mosquitoes of i-genotypes occurs at a rate $\mu_m^i(\mu_f^i)$. Exposed adult female mosquitoes of each genotype become infectious at a rate θ_i (with $i = SS,\ RS,\ RR$).

2.2.3. Humans

The differential equations for the dynamics of malaria in the human host population are given by:

$$\begin{aligned}
\frac{dS_{H_p}}{dt} &= C_B\Pi_H + \xi_H R_{H_p} - (\lambda_{VH}^{p^{SS}} + \lambda_{VH}^{p^{RS}} + \lambda_{VH}^{p^{RR}})S_{H_p} - \mu_H S_{H_p},\\
\frac{dE_{H_p}}{dt} &= (\lambda_{VH}^{p^{SS}} + \lambda_{VH}^{p^{RS}} + \lambda_{VH}^{p^{RR}})S_{H_p} - (\sigma_H + \mu_H)E_{H_p},\\
\frac{dI_{H_p}}{dt} &= \sigma_H E_{H_p} - (\gamma_H + \mu_H + \delta_H)I_{H_p},\\
\frac{dR_{H_p}}{dt} &= \gamma_H I_{H_p} - (\xi_H + \mu_H)R_{H_p},\\
\frac{dS_{H_u}}{dt} &= (1-C_B)\Pi_H + \xi_H R_{H_u} - \lambda_{VH}^{u}S_{H_u} - \mu_H S_{H_u},\\
\frac{dE_{H_u}}{dt} &= \lambda_{VH}^{u}S_{H_u} - (\sigma_H + \mu_H)E_{H_u},\\
\frac{dI_{H_u}}{dt} &= \sigma_H E_{H_u} - (\gamma_H + \mu_H + \delta_H)I_{H_u},\\
\frac{dR_{H_u}}{dt} &= \gamma_H I_{H_u} - (\xi_H + \mu_H)R_{H_u}.
\end{aligned} \tag{2.10}$$

In (2.10), Π_H is the human recruitment rate (due to immigration or birth) and C_B is the proportion of protected humans. The parameter ξ_H represents the rate of loss of temporary immunity acquired from prior malaria infection (i.e., the rate at which recovered humans become fully susceptible again). Susceptible unprotected (protected)-humans acquire malaria infection, following effective contact with an infected female *Anopheles* mosquito (of i-genotype), at a rate $\lambda_{HV}^{u}(\lambda_{HV}^{p^i})$. Humans in all epidemiological compartments are assumed to suffer natural death at a rate μ_H. Exposed humans develop clinical symptoms of malaria, and become infectious, at a rate of σ_H. Infectious humans recover (naturally) at a rate of γ_H. A schematic diagram of the model is depicted in Fig. 1, and the state variables and parameters of the model are described in Tables 1–4. The model {(2.5)–(2.10)} is an extension of several models that study the spread of insecticide resistance in vectors (in response to the community wide use of chemical insecticides, such as ITNs, IRS, or larvicide) and/or its impact on disease dynamics (such as those in [15,22,29–31,44–47]) by, *inter alia*:

i. coupling malaria epidemiology in humans (by including the dynamics of mosquito populations and humans) and population genetics (malaria epidemiology and genetics are not simultaneously considered in [15,22,29–31,44–47]). This allows us to investigate the disease dynamics and evolution of insecticide resistance simultaneously (epidemiology and population genetics are not simultaneously included in the models in [15,30,31,44–47]);
ii. explicitly incorporating the dynamics of aquatic/immature mosquitoes (these are not included in the population genetic models in [15,30,31], or in the population-level mathematical models in [15,30,31,44,45,47], or in the coupled model in [22, 29]): incorporating this feature allows us to realistically model the impact of larvicides on the spread of insecticide resistance and the disease (these are not included in the population genetic models in [15,30,31], or in the population-level mathematical models in [15,30,31,44,45,47], or in the coupled epidemiology-genetic model in [22,29]);
iii. explicitly including the dynamics of the male mosquito population (these are not included in the population genetic model in [31], or in the population-level mathematical models in [31,44, 45,47], or in the coupled epidemiology-genetic model in [22,29]);
iv. incorporating the fitness cost of resistance by reducing fecundity (growth rate) and increasing natural mortality in heterozygous and homozygous resistant mosquitoes (these are not included in the models in [31,44,45,47]);
v. incorporating a parameter for the level of dominance (h) that measures of the relative position of the RS-genotype relative to the SS- and RR-genotypes in terms of their sensitivity to insecticide (this is not included in the models in [29,31,44–47]).

Furthermore, the model {(2.5)–(2.10)} extends the coupled epidemiology-genetic model in [22] by:

(a) including the dynamics of aquatic/immature mosquitoes (this is not included in [22]). This enables us to realistically investigate the impact of vector controls at aquatic stage (such as larvicides) on the spread of insecticide resistance and the disease;
(b) including the dynamics of male mosquitoes in the model {(2.5)–(2.10)} (this is not included in [22]). This enables us to explicitly include the fitness costs/benefits of resistance alleles in the male mosquito to malaria epidemiology and to investigate their impact in the evolution of insecticide resistance and spread of the disease;
(c) incorporating protected (unprotected) human compartments in accordance to their bednets usage (i.e., whether or not they sleep under an LLIN). This was not incorporated in the model in [22],

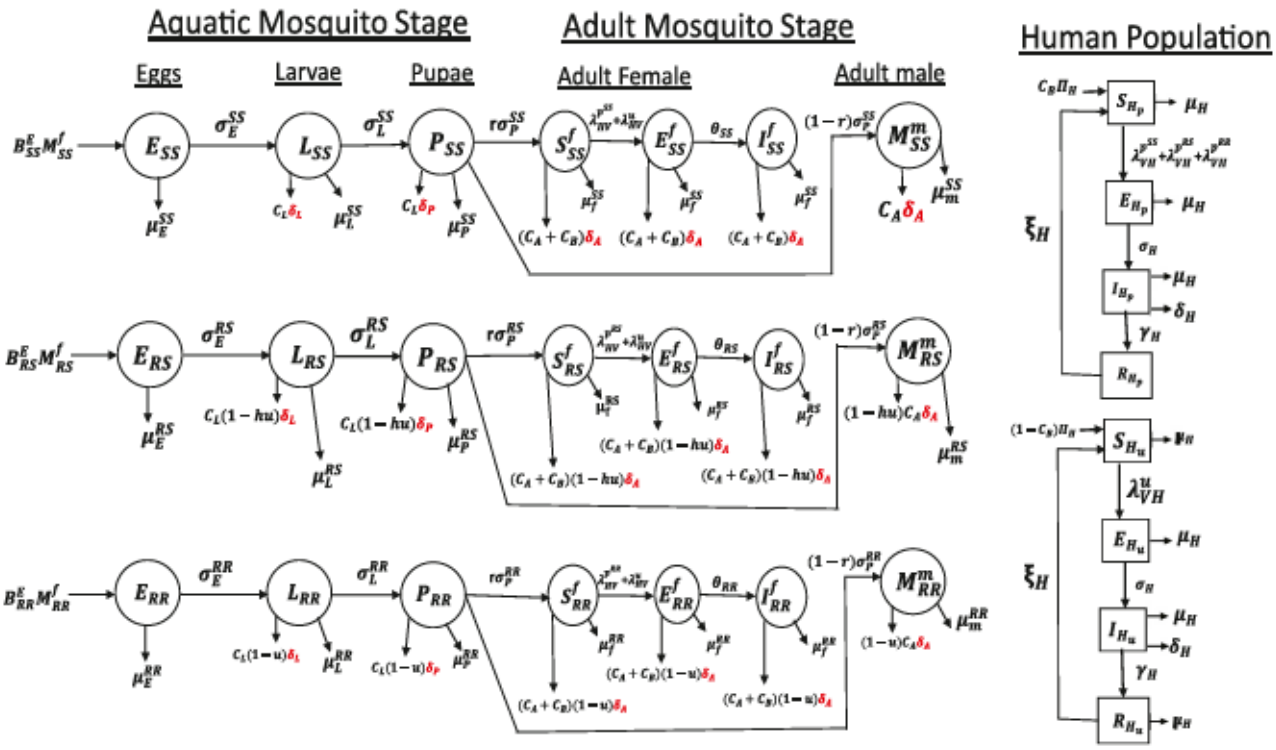

Fig. 1. Flow diagram of the model {(2.5)–(2.10)}, where B^E_{SS}, B^E_{RS} and B^E_{RR} are given, respectively, by $B^E_{SS}(t) = \psi q_f(t) q_m(t) \left(1 - \frac{\pi(t)}{\kappa_z}\right)_+$, $B^E_{RS}(t) = \psi \left[q_f(t) p_m(t) + q_m(t) p_f(t)\right] \left(1 - \frac{\pi(t)}{\kappa_z}\right)_+$ and $B^E_{RR}(t) = \psi p_f(t) p_m(t) \left(1 - \frac{\pi(t)}{\kappa_z}\right)_+$.

humans were stratified as those who use LLINs properly (low-risk group) and those who do not (high-risk group). Incorporating this feature allows us to monitor changes in disease burden as a function of LLIN coverage and efficacy;

(d) incorporating a new non-linear genotype-specific mosquito biting rate function (b_l), which depends on LLINs coverage (C_B) and genotype-specific LLINs efficacy (ϵ^i_B, where $i = SS, RS, RR$) into the developed model {(2.5)–(2.10)} (linear biting rates were used in [22,36,41,48–51], and no genotype-specific LLINs efficacy is incorporated in [41,48–51]). Adding this novel feature into the developed model allows us to investigate the impact of the non-linear relationship between bednets coverage and the mosquito genotype-dependent bednets efficacy (in addition to adding realism to the modeling of malaria transmission dynamics).

2.3. Basic properties

The basic qualitative properties of the model {(2.5)–(2.10)} are explored in this section, with the positivity and boundedness of the solutions of the model established. It is convenient to group the variables of the model {(2.5)–(2.10)} as follows:

$$\begin{aligned} B_1 &= \left(E_{SS}, L_{SS}, P_{SS}, E_{RS}, L_{RS}, P_{RS}, E_{RR}, L_{RR}, P_{RR}\right), \\ B_2 &= \left(S^f_{SS}, E^f_{SS}, I^f_{SS}, M^m_{SS}\right), \\ B_3 &= \left(S^f_{RS}, E^f_{RS}, I^f_{RS}, M^m_{RS}\right), \ B_4 = \left(S^f_{RR}, E^f_{RR}, I^f_{RR}, M^m_{RR}\right), \\ B_5 &= \left(S_{H_p}, E_{H_p}, I_{H_p}, R_{H_p}, S_{H_u}, E_{H_u}, I_{H_u}, R_{H_u}\right). \end{aligned} \tag{2.11}$$

Consider the feasible region $\Omega = \Omega_1 \cup \Omega_2 \cup \Omega_3 \cup \Omega_4 \cup \Omega_5$ and the variables $B(t) = B_1(t) \cup B_2(t) \cup B_3(t) \cup B_4(t) \cup B_5(t)$ of the model {(2.5)–(2.10)}, where:

$$\begin{aligned} \Omega_1 = \big\{ & B_1 \in \mathbb{R}^9_+ : E_{SS} \le K_E, L_{SS} \le L^\circ_{SS}, P_{SS} \le P^\circ_{SS}, E_{RS} \le K_E, \\ & L_{RS} \le L^\circ_{RS}, P_{RS} \le P^\circ_{RS}, E_{RR} \le K_E, L_{RR} \le L^\circ_{RR}, P_{RR} \le P^\circ_{RR} \big\}, \end{aligned}$$

$$\begin{aligned} \Omega_2 &= \left\{ B_2 \in \mathbb{R}^4_+ : A_{SS}(t) \le \frac{r\sigma^{SS}_P P^\circ_{SS}}{Q_1} \right\}, \\ \Omega_3 &= \left\{ B_3 \in \mathbb{R}^4_+ : A_{RS}(t) \le \frac{r\sigma^{RS}_P P^\circ_{RS}}{Q_2} \right\}, \\ \Omega_4 &= \left\{ B_4 \in \mathbb{R}^4_+ : A_{RR}(t) \le \frac{r\sigma^{RR}_P P^\circ_{RR}}{Q_3} \right\}, \\ \Omega_5 &= \left\{ B_5 \in \mathbb{R}^8_+ : N_H(t) \le \frac{\Pi_H}{\mu_H} \right\}, \end{aligned} \tag{2.12}$$

with,

$$\begin{aligned} L^\circ_{SS} &= \frac{\sigma^{SS}_E K_E}{K_1}, \ P^\circ_{SS} = \frac{\sigma^{SS}_L L^\circ_{SS}}{K_4}, \ L^\circ_{RS} = \frac{\sigma^{RS}_E K_E}{K_2}, \ P^\circ_{RS} = \frac{\sigma^{RS}_L L^\circ_{RS}}{K_5}, \\ L^\circ_{RR} &= \frac{\sigma^{RR}_E K_E}{K_3}, \ P^\circ_{RR} = \frac{\sigma^{RR}_L L^\circ_{RR}}{K_6}, \\ K_1 &= \sigma^{SS}_E + \mu^{SS}_E, \ K_2 = \sigma^{RS}_E + \mu^{RS}_E, \ K_3 = \sigma^{RR}_E + \mu^{RR}_E, \\ K_4 &= \sigma^{SS}_L + \mu^{SS}_L + \varepsilon_L C_L \delta_L, \\ K_5 &= \sigma^{RS}_L + \mu^{RS}_L + \varepsilon_L C_L (1 - hu)\delta_L, \ K_6 = \sigma^{RR}_L + \mu^{RR}_L + \varepsilon_L C_L (1 - u)\delta_L, \\ K_7 &= \sigma^{SS}_P + \mu^{SS}_P + \varepsilon_L C_L \delta_P, \ K_8 = \sigma^{RS}_P + \mu^{RS}_P + \varepsilon_L C_L (1 - hu)\delta_P, \\ K_9 &= \sigma^{RR}_P + \mu^{RR}_P + \varepsilon_L C_L (1 - u)\delta_P, \\ K_{10} &= \mu^{SS}_m + \delta_A \varepsilon_A C_A, \ K_{11} = \mu^{RS}_m + (1 - hu)\delta_A \varepsilon_A C_A, \\ K_{12} &= \mu^{RR}_m + (1 - u)\delta_A \varepsilon_A C_A, \\ K_{13} &= \mu^{SS}_f + \delta_A \varepsilon_A (C_A + C_B), \ K_{14} = \theta_{SS} + \mu^{SS}_f + \delta_A \varepsilon_A (C_A + C_B), \\ K_{15} &= \mu^{RS}_f + (1 - hu)\delta_A \varepsilon_A (C_A + C_B), \\ K_{16} &= \theta_{RS} + \mu^{RS}_f + (1 - hu)\delta_A \varepsilon_A (C_A + C_B), \\ K_{17} &= \mu^{RR}_f + (1 - u)\delta_A \varepsilon_A (C_A + C_B), \\ K_{18} &= \theta_{RR} + \mu^{RR}_f + (1 - u)\delta_A \varepsilon_A (C_A + C_B), \ K_{19} = \sigma_H + \mu_H, \\ K_{20} &= \gamma_H + \delta_H + \mu_H, \ K_{21} = \xi_H + \mu_H, \\ Q_1 &= \min\{K_{10}, K_{13}\}, \ Q_2 = \min\{K_{11}, K_{15}\} \text{ and } Q_3 = \min\{K_{12}, K_{17}\}. \end{aligned}$$

Table 1
Description of insecticide-independent mosquito-related parameters of the model {(2.5)–(2.10)}.

Parameters	Interpretation	Range (day^{-1})	Baseline (day^{-1})	Reference
Immature mosquitoes				
ψ	Production (laying) rate of eggs of all genotypes	0.5–4	4	[24,38]
K_E	Environmental carrying capacity of eggs	$10^6 - 10^8$	1×10^7	[22,39]
μ_E^{SS}	Mortality rate of eggs of SS-genotype	0.0608–0.0912	0.0760	[24]
μ_E^{RS}	Mortality rate of eggs of RS-genotype	0.076–0.114	$1.25\times\mu_E^{SS}$	[22,24]
μ_E^{RR}	Mortality rate of eggs of RR-genotype	0.1064–0.1596	$1.75\times\mu_E^{SS}$	[22,24]
μ_L^{SS}	Mortality rate of larvae of SS-genotype	0.0608–0.0912	0.0760	[24]
μ_L^{RS}	Mortality rate of larvae of RS-genotype	0.076–0.114	$1.25\times\mu_L^{SS}$	[22,24]
μ_L^{RR}	Mortality rate of larvae of RR-genotype	0.1064–0.1596	$1.75\times\mu_L^{SS}$	[22,24]
μ_P^{SS}	Mortality rate of pupae of SS-genotype	0.0608–0.0912	0.0760	[24]
μ_P^{RS}	Mortality rate of pupae of RS-genotype	0.076–0.114	$1.25\times\mu_P^{SS}$	[22,24]
μ_P^{RR}	Mortality rate of pupae of RR-genotype	0.1064–0.1596	$1.75\times\mu_P^{SS}$	[22,24]
σ_E^{SS}	Development rate from eggs to larvae of SS-genotype	0.33 – 1	0.5	[24,38]
σ_E^{RS}	Development rate from eggs to larvae of RS-genotype	0.264–0.8	$\frac{1}{1.25}\times\sigma_E^{SS}$	[22,24,38]
σ_E^{RR}	Development rate from eggs to larvae of RR-genotype	0.189–0.571	$\frac{1}{1.75}\times\sigma_E^{SS}$	[22,24,38]
σ_L^{SS}	Development rate from larvae to pupae and of SS-genotype	0.33 – 1	0.14	[24,38]
σ_L^{RS}	Development rate from larvae to pupae and of RS-genotype	0.264–0.8	$\frac{1}{1.25}\times\sigma_L^{SS}$	[22,24,38]
σ_L^{RR}	Development rate from larvae to pupae and of RR-genotype	0.189–0.571	$\frac{1}{1.75}\times\sigma_L^{SS}$	[22,24,38]
σ_P^{SS}	Development rate from pupae to adult mosquitoes of SS-genotype	0.33 – 1	0.5	[24,38]
σ_P^{RS}	Development rate from pupae to adult mosquitoes of RS-genotype	0.264–0.8	$\frac{1}{1.25}\times\sigma_P^{SS}$	[22,24,38]
σ_P^{RR}	Development rate from pupae to adult mosquitoes of RR-genotype	0.189–0.571	$\frac{1}{1.75}\times\sigma_P^{SS}$	[22,24,38]
Adult mosquitoes				
r	Proportion of new adult mosquitoes that are females	0.5–0.8(dimensionless)	0.5	[22,24,38]
μ_m^{SS}	Natural death rate of adult male mosquitoes of SS-genotypes	$\frac{1}{21}-\frac{1}{14}$	$\frac{1}{7}$	[40]
μ_m^{RS}	Natural death rate of adult male mosquitoes of RS-genotypes	$\frac{5}{84}-\frac{5}{56}$	$1.25\times\mu_m^{SS}$	[22,41]
μ_m^{RR}	Natural death rate of adult male mosquitoes of RR-genotypes	$\frac{7}{84}-\frac{7}{56}$	$1.75\times\mu_m^{SS}$	[22,41]
μ_f^{SS}	Natural death rate of adult female mosquitoes of SS-genotypes	$\frac{1}{21}-\frac{1}{14}$	$\frac{1}{14}$	[41]
μ_f^{RS}	Natural death rate of adult female mosquitoes of RS-genotypes	$\frac{5}{84}-\frac{5}{56}$	$1.25\times\mu_f^{SS}$	[22,41]
μ_f^{RR}	Natural death rate of adult female mosquitoes of RR-genotypes	$\frac{7}{84}-\frac{7}{56}$	$1.75\times\mu_f^{SS}$	[22,41]
θ_{SS}	Progression rate of exposed adult female mosquitoes of SS-genotype to infectious stage	0–0.1	0.1	[24,38]
θ_{RS}	Progression rate of exposed adult female mosquitoes of RS-genotype to infectious stage	0–0.125	$1.25\times\theta_{SS}$	[22,24,38]
θ_{RR}	Progression rate of exposed adult female mosquitoes of RR-genotype to infectious stage	0–0.175	$1.75\times\theta_{SS}$	[22,24,38]
b_{max}	Maximum adult mosquito biting rate	0–4	2	[22,30]
β_V	Transmission probability from infectious humans to susceptible mosquitoes	0.02–0.05	0.48	[22]

Lemma 2.1. *Each component of the solution of the model {(2.5)–(2.10)}, subject to non-negative initial conditions, remains non-negative and bounded for all $t > 0$.*

Proof. It should be noted, first of all, that the right-hand side of each of the equations of the model {(2.5)–(2.10)} is continuous and locally-Lipschitz at $t = 0$. Hence, a solution of the model with non-negative initial conditions exists and is unique in Ω for all time $t > 0$ (see also [24,38]). Furthermore, since $\left(1-\frac{E(t)}{K_E}\right)_+ \geq 0$, it follows from the sub-system (2.5) that $E(t) \leq K_E$ for all time $t > 0$. Thus, it follows from (2.1) that $E_{SS}(t0) \leq K_E$, $E_{RS}(t) \leq K_E$, and $E_{RR}(t) \leq K_E$ for all $t \geq 0$. Similarly, it follows from the second sub-system (2.6) that (where a dot represents differentiation with respect to time t)

$$\dot{L}_{SS} = \sigma_E^{SS}E_{SS} - (\sigma_L^{SS} + C_L\delta_L + \mu_L^{SS})L_{SS} \leq \sigma_E^{SS}K_E - (\sigma_L^{SS} + C_L\delta_L + \mu_L^{SS})L_{SS},$$

so that $\limsup_{t\to\infty} L_{SS}(t) \leq \frac{\sigma_E^{SS}K_E}{K_1} = L_{SS}^*$. Using a similar approach, it can be shown that $\limsup_{t\to\infty} L_{RS}(t) \leq \frac{\sigma_E^{RS}K_E}{K_2} = L_{RS}^*$, $\limsup_{t\to\infty} L_{RR}(t) \leq \frac{\sigma_E^{RR}K_E}{K_3} = L_{RR}^*$, $\limsup_{t\to\infty} P_{SS}^\circ \leq \frac{\sigma_L^{SS}L_{SS}^*}{K_4} = P_{SS}^*$, $\limsup_{t\to\infty} P_{RS}^\circ \leq \frac{\sigma_L^{RS}L_{RS}^*}{K_5} = P_{RS}^*$, and $\limsup_{t\to\infty} P_{RR}^\circ \leq \frac{\sigma_L^{RR}L_{RS}^*}{K_6} = P_{RR}^*$. That is, all solutions of the sub-system (2.7) are bounded for all time $t > 0$.

For the boundedness of the solutions of the sub-systems (2.8) and (2.9), we consider the following equations (for the rate of change of the total adult mosquito populations by genotype):

$$\begin{aligned}\dot{A}_{SS} &= \sigma_P^{SS}P_{SS} - Q_1A_{SS} \leq \sigma_P^{SS}P_{SS}^\circ - Q_1A_{SS},\\ \dot{A}_{RS} &= \sigma_P^{RS}P_{RS} - Q_2A_{RS} \leq \sigma_P^{RS}P_{RS}^\circ - Q_2A_{RS},\\ \dot{A}_{RR} &= \sigma_P^{RR}P_{RR} - Q_3A_{RR} \leq \sigma_P^{RR}P_{RR}^\circ - Q_3A_{RR},\end{aligned} \tag{2.13}$$

where, $A_{SS} = S_{SS}^f + E_{SS}^f + I_{SS}^f + M_{SS}^m$, $A_{RS} = S_{RS}^f + E_{RS}^f + I_{RS}^f + M_{RS}^m$ and $A_{RR} = S_{RR}^f + E_{RR}^f + I_{RR}^f + M_{RR}^m$. It follows from (2.13) that

$$\limsup_{t\to\infty} A_{SS}(t) \leq \frac{\sigma_P^{SS}P_{SS}^\circ}{Q_1},\ \limsup_{t\to\infty} A_{RS}(t) \leq \frac{\sigma_P^{RS}P_{RS}^\circ}{Q_2} \text{ and } \limsup_{t\to\infty} A_{RR}(t) \leq \frac{\sigma_P^{RR}P_{RR}^\circ}{Q_3}. \tag{2.14}$$

Hence, the solutions of the equations of the sub-system (2.9) are bounded for all time $t > 0$.

Finally, consider the equation for the rate of change of the total human population, given by:

$$\dot{N}_H = \Pi_H - \mu_H N_H - \delta_H(I_{H_p} + I_{H_u}) \leq \Pi_H - \mu_H N_H, \tag{2.15}$$

from which it follows that $\limsup_{t\to\infty} N(t) \leq \frac{\Pi_H}{\mu_H}$. Thus, the solutions of the sub-system (2.10) are bounded for all $t > 0$. Since the solutions

Table 2
Description of insecticide-dependent mosquito-related parameters of the model {(2.5)–(2.10)}.

Parameters	Interpretation	Range (day^{-1})	Baseline (day^{-1})	Ref.
Immature mosquitoes				
δ_L	Larvicide-induced death rate for larvae	0.672–1.01	0.84	
δ_P	Larvicide-induced death rate for pupae	0.672–1.01	0.84	
δ_A	Insecticide-induced death rate for adult mosquitoes	0.672–1.01	0.84	[22,30]
Adult mosquitoes				
u	Modification parameter accounting for the assumed decrease in the mortality rate of adult mosquitoes of RR-genotype due to the use of insecticides (larvicides and adulticides), in comparison to insecticide-induced mortality rate of adult mosquitoes with SS-genotype ($0 \le u \le 1$)	$0-1$	Varied	[22]
h	Modification parameter accounting for the measure of the dominance of the resistant allele over the sensitive allele ($0 \le h \le 1$)	$0-1$ (dimensionless)	0.9	[22,30]
C_A	Proportion of houses (indoors) sprayed with adulticides ($0 \le C_A \le 1$)	0-1(dimensionless)	0.25	[22,30]
C_L	Proportion of mosquito breeding sites sprayed with larvicides	$0-1$(dimensionless)	Varied	
ε_A	Efficacy of adulticides ($0 \le \varepsilon_A \le 1$)	$0-1$ (dimensionless)	Varied	
ε_L	Efficacy of larvicides ($0 \le \varepsilon_L \le 1$)	$0-1$ (dimensionless)	0.85	[42]
ε_B^{SS}	Efficacy of LLINs ($0 \le \varepsilon_B \le 1$) to protect humans from bites by mosquitoes of SS-genotype	$0-1$ (dimensionless)	0.85	[42]
ε_B^{RS}	Efficacy of LLINs ($0 \le \varepsilon_B \le 1$) to protect humans from bites by mosquitoes of RS-genotype	0.2 – 1 (dimensionless)	0.85	Estimated [43]
ε_B^{RR}	Efficacy of LLINs ($0 \le \varepsilon_B \le 1$) to protect humans from bites by mosquitoes of RR-genotype	$0-1$ (dimensionless)	$\frac{1}{1.25}\varepsilon_B^{ss}$	Estimated [43]
$b_i (i = SS, RS, RR)$	Average biting rate for mosquitoes of i-genotype	$0 \le b_i \le b_{max}$	$\frac{1}{1.75}\varepsilon_B^{ss}$	Estimated [43]
			Varied	Computed based on values of ε_B^i, C_B and b_{max}

Table 3
Description of human-related parameters of the model {(2.5)–(2.10)}.

Parameters	Interpretation	Range (day^{-1})	Baseline (day^{-1})	Ref.
Π_H	Human recruitment rate (due to birth or immigration)	2–5.5	2.19	[22,38]
C_B	Proportion of humans who use bednets (LLINs) ($0 \le C_B \le 1$)	$0-1$(dimensionless)	Varied	
β_H	Transmission probability from infectious mosquitoes to susceptible humans	0.01–0.05 (dimensionless)	0.14	[22]
μ_H	Natural death rate for humans	$1/(50\times 365) - 1/(70\times 365)$	$1/(60\times 365)$	[38]
δ_H	Disease-induced death rate for humans	$7.2^{-5} - 1.08\times 10^{-4}$	9×10^{-5}	[22]
σ_H	Rate of development of clinical symptoms of malaria	$1/17 - 1/14$	1/14	[22,38]
ξ_H	Rate of loss of natural immunity for humans		5.6×10^{-3}	[22]
γ_H	Recovery rate for humans	$1/1500 - 1/100$	1/30	[24,38]

Table 4
Description of state variables and forces of infection of the model {(2.5)–(2.10)}.

State variable, $i = \{SS, RS, RR\}$	Interpretation
E_i	Number of eggs of i-genotype
L_i	Number of larvae of i-genotype
P_i	Number of pupae of i-genotype
S_i^f	Number of susceptible female mosquitoes of i-genotype
E_i^f	Number of exposed female mosquitoes of i-genotype
I_i^f	Number of infectious female mosquitoes of i-genotype
M_i^f	Total number of adult female mosquitoes of i-genotype
M_i^m	Population of adult male mosquitoes of i-genotype
$S_{Hp}(S_{Hu})$	Number of protected (unprotected) susceptible humans
$E_{Hp}(E_{Hu})$	Number of protected (unprotected) exposed (infected but not yet infectious) humans
$I_{Hp}(I_{Hu})$	Number of protected (unprotected) infectious (symptomatic) humans
$R_{Hp}(R_{Hu})$	Number of protected (unprotected) recovered humans
Force of infection, $i = \{SS, RS, RR\}$	**Interpretation**
$\lambda_{HV}^u(\lambda_{HV}^p)$	Unprotected (protected)-human-to-vector (of i-genotype) malaria transmission rate
$\lambda_{VH}^u(\lambda_{VH}^p)$	Vector (of i-genotype)-to-unprotected (protected)-human malaria transmission rate

of the three sub-systems of the model {(2.5)–(2.10)} are bounded, it follows that the solutions of the full model {(2.5)–(2.10)} are also bounded. □

Theorem 2.1. *The region Ω is positively-invariant and attracts all solutions of the model {(2.5)–(2.10)}.*

Proof. The proof for the invariance of the region Ω_1 follows from the bounds established in Lemma 2.1 and the fact that $\dot{E}(t) < 0$ whenever $E(t) > K_E$, $\dot{L}_{SS}(t) < 0$ whenever $L_{SS}(t) > L_{SS}^*$ and $\dot{L}_i(t) < 0$ whenever $L_i(t) > L_i^*$ $(i = RS, RR)$, respectively. For the invariance of the regions Ω_2, Ω_3 and Ω_4, it can be seen from the equations in (2.13) that $\dot{A}_{SS} < 0$ whenever $A_{SS}(t) > \frac{\sigma^{SS} P_{SS}^*}{Q_1}$, $\dot{A}_{RS} < 0$ whenever $A_{RS}(t) > \frac{\sigma^{RS} P_{RS}^*}{Q_2}$ and

$A_{RR} < 0$ whenever $A_{RR}(t) > \frac{\sigma^{RR}_P P^*_{RR}}{Q_3}$, for all $t > 0$. Finally, it follows from the equation for the rate of change of the total human population (2.15) that $\dot{N}_H < 0$ whenever $N_H(t) > \frac{\Pi_H}{\mu_H}$. Thus, the region Ω_5 is invariant with respect to the sub-system (2.10) of the model {(2.5)–(2.10)}. Since the sub-regions $\Omega_i (i = 1, 2, 3, 4, 5)$ are positively-invariant and attracting with respect to the model {(2.5)–(2.10)}, it follows that the region Ω is positively-invariant and attracting with respect to the model {(2.5)–(2.10)}. □

3. Existence and asymptotic stability of disease-free equilibria

In this section, the existence and asymptotic stability property of the disease-free equilibria of the model {(2.5)–(2.10)} will be explored.

3.1. Existence of disease-free equilibria

It is convenient, first of all, to define the following:

$$\mathcal{R}_{SS} = \frac{r\psi\sigma_E^{SS}\sigma_L^{SS}\sigma_P^{SS}}{K_1K_4K_7K_{13}},\ \mathcal{R}_{RS} = \frac{r\psi\sigma_E^{RS}\sigma_L^{RS}\sigma_P^{RS}}{K_2K_5K_8K_{15}} \text{ and}$$
$$\mathcal{R}_{RR} = \frac{r\psi\sigma_E^{RR}\sigma_L^{RR}\sigma_P^{RR}}{K_3K_6K_9K_{17}}. \tag{3.1}$$

The threshold quantity $\mathcal{R}_i$ (for $i = SS, RS, RR$) represents the average number of adult mosquitoes of genotype-i produced by an adult female mosquito of the same genotype during its lifetime.

The model {(2.5)–(2.10)} has the following disease-free equilibria:

(i) Trivial disease-free equilibrium ($TDFE$), given by:

$$\mathcal{T}_1 = \Big(0,0,0,0,0,0,0,0,0,0,0,0,0,0,0,0,0,0,0,0,0,0,$$
$$S^0_{H_p},0,0,0,S^0_{H_u},0,0,0\Big),$$
$$= \Big(0,0,0,0,0,0,0,0,0,0,0,0,0,0,0,0,0,0,0,0,0,0,\frac{C_B\Pi_H}{\mu_H},0,0,0,$$
$$\times\frac{(1-C_B)\Pi_H}{\mu_H},0,0,0\Big).$$

The equilibrium $\mathcal{T}_1$ is ecologically unrealistic (since it is associated with the total absence of mosquitoes in the community). Hence, it is not qualitatively analyzed.

(ii) Non-trivial sensitive-only disease-free equilibrium ($NTSDFE$), given by:

$$\mathcal{T}_2 = \Big(E^*_{SS},0,0,L^*_{SS},0,0,P^*_{SS},0,0,M^{m*}_{SS},0,0,S^{f*}_{SS},0,0,0,0,0,0,0,0,$$
$$\frac{C_B\Pi_H}{\mu_H},0,0,0,\frac{(1-C_B)\Pi_H}{\mu_H},0,0,0\Big),$$

where,

$$E^*_{SS} = \frac{K_E}{\mathcal{R}_{SS}}\left(\mathcal{R}_{SS}-1\right),\ L^*_{SS} = \frac{\sigma_E^{SS}E^*_{SS}}{K_4},\ P^*_{SS} = \frac{\sigma_L^{SS}L^*_{SS}}{K_7},$$
$$M^{m*}_{SS} = \frac{(1-r)\sigma_P^{SS}P^*_{SS}}{K_{10}} \text{ and } S^{f*}_{SS} = \frac{r\sigma_P^{SS}P^*_{SS}}{K_{13}}.$$

(iii) Non-trivial resistance-only disease-free equilibrium ($NTRDFE$), given by:

$$\mathcal{T}_3 = \Big(0,0,E^{**}_{RR},0,0,L^{**}_{RR},0,P^{**}_{RS},P^{**}_{RR},0,0,M^{m**}_{RR},0,0,S^{f**}_{RR},0,0,0,$$
$$0,0,0,\frac{C_B\Pi_H}{\mu_H},0,0,0,\frac{(1-C_B)\Pi_H}{\mu_H},0,0,0\Big),$$

where,

$$E^{**}_{RR} = \frac{K_E}{\mathcal{R}_{RR}}\left(\mathcal{R}_{RR}-1\right),\ L^{**}_{RR} = \frac{\sigma_E^{RR}E^{**}_{RR}}{K_6},\ P^{**}_{RR} = \frac{\sigma_L^{RR}L^{**}_{RR}}{K_9},$$
$$M^{m**}_{RR} = \frac{(1-r)\sigma_P^{RR}P^{**}_{RR}}{K_{12}} \text{ and } S^{f**}_{RR} = \frac{r\sigma_P^{RR}P^{**}_{RR}}{K_{17}}.$$

(iv) Non-trivial co-existence disease-free equilibrium ($NTCDFE$), given by:

$$\mathcal{T}_4 = \Big(E^{***}_{SS},E^{***}_{RS},E^{***}_{RR},L^{***}_{SS},L^{***}_{RS},L^{***}_{RR},P^{***}_{SS},P^{***}_{RS},P^{***}_{RR},M^{m***}_{SS},$$
$$M^{m***}_{RS},M^{m***}_{RR},S^{f***}_{SS},0,0,S^{f***}_{RS},0,0,S^{f***}_{RR},$$
$$0,0,\frac{\xi\Pi}{\mu_H},0,0,0,\frac{(1-\xi)\Pi}{\mu_H},0,0,0\Big),$$

where,

$$M^{m***}_{SS} > 0,\ M^{m***}_{RS} > 0,\ M^{m***}_{RR} > 0,\ S^{f***}_{SS} > 0,\ S^{f***}_{RS} > 0,\ S^{f***}_{RR} > 0,$$
$$E^{***}_{SS} = \frac{K_EK_2K_3q_f^{***}q_m^{***}(\mathcal{R}_C-1)}{\mathcal{R}^*_C\mathcal{R}_C},\ E^{***}_{RS} = \frac{K_1}{K_2}\left(\frac{p_f^{***}}{q_f^{***}}+\frac{p_m^{***}}{q_m^{***}}\right)E^{***}_{SS},$$
$$E^{***}_{RR} = \frac{K_1}{K_3}\frac{p_f^{***}p_m^{***}}{q_f^{***}q_m^{***}}E^{***}_{SS},\ L^{***}_{SS} = \frac{s_E^{SS}}{K_4}E^{***}_{SS},\ L^{***}_{RS} = \frac{s_E^{RS}}{K_5}E^{***}_{RS},$$
$$L^{***}_{RR} = \frac{s_E^{RR}}{K_6}E^{***}_{RR}, \tag{3.2}$$
$$P^{***}_{SS} = \frac{\sigma_L^{SS}}{K_7}L^{***}_{SS},\ P^{***}_{RS} = \frac{\sigma_L^{RS}}{K_8}L^{***}_{RS},\ P^{***}_{RR} = \frac{\sigma_L^{RR}}{K_9}L^{***}_{RR},$$

with,

$$q_f^{***} = \frac{S^{f***}_{SS}+\frac{1}{2}S^{f***}_{RS}}{S^{f***}_{SS}+S^{f***}_{RS}+S^{f***}_{RR}},\ p_f^{***} = \frac{S^{f***}_{RR}+\frac{1}{2}S^{f***}_{RS}}{S^{f***}_{SS}+S^{f***}_{RS}+S^{f***}_{RR}},$$
$$q_m^{***} = \frac{M^{m***}_{SS}+\frac{1}{2}M^{m***}_{RS}}{M^{m***}_{SS}+M^{m***}_{RS}+M^{m***}_{RR}},$$
$$p_m^{***} = \frac{M^{m***}_{RR}+\frac{1}{2}M^{m***}_{RS}}{M^{m***}_{SS}+M^{m***}_{RS}+M^{m***}_{RR}}, \tag{3.3}$$
$$\mathcal{R}_C = \mathcal{R}_{SS}q_f^{***}q_m^{***}+\mathcal{R}_{RS}(p_f^{***}q_m^{***}+p_m^{***}q_f^{***})+\mathcal{R}_{RR}p_f^{***}p_m^{***},$$
$$\mathcal{R}^*_C = K_2K_3q_f^{***}q_m^{***}+K_1K_3(p_f^{***}q_m^{***}+p_m^{***}q_f^{***})+K_1K_2p_f^{***}p_m^{***}.$$

The results below follow from the expressions and inequalities given in {(3.2), (3.3)}.

Theorem 3.1. *The model {(2.5)–(2.10)} has a:*

(i) Trivial disease-free equilibrium ($\mathcal{T}_1$), which always exists.
(ii) Non-trivial sensitive-only disease-free equilibrium ($\mathcal{T}_2$) if and only if $\mathcal{R}_{SS} > 1$.
(iii) Non-trivial resistant-only disease-free equilibrium ($\mathcal{T}_3$) if and only if $\mathcal{R}_{RR} > 1$.
(iv) Non-trivial co-existence disease-free equilibrium ($\mathcal{T}_4$) if and only if $0 < p_i^{***}, q_i^{***} < 1$ $(i = f, m)$ and $\mathcal{R}_C > 1$.

3.2. Asymptotic stability of disease-free equilibria

Let, without loss of generality, $\mathcal{T}_4$ be a generalized non-trivial disease-free equilibrium of the model {(2.5)–(2.10)} (it should be noted that each of the other three disease-free equilibria of the model, $\mathcal{T}_1$, $\mathcal{T}_2$ and $\mathcal{T}_3$, can be recovered from $\mathcal{T}_4$).

3.2.1. Local asymptotic stability

The linear stability of the generalized non-trivial disease-free equilibrium $\mathcal{T}_4$ of the model {(2.5)–(2.10)} can be established using the next generation operator method [52,53] on the model {(2.5)–(2.10)}. The following ordering is used for the infected compartments: $\left(E^f_{SS}, I^f_{SS}, E^f_{RS}, I^f_{RS}, E^f_{RR}, I^f_{RR}, E_{H_p}, I_{H_p}, E_{H_u}, I_{H_u}\right)$. Using the notation in [53], the next generation matrices, F and V for the new infection terms and the remaining transfer terms, are given, respectively, F in Box I,

$$F=\begin{bmatrix}
0 & 0 & 0 & 0 & 0 & 0 & 0 & \frac{\beta_V\mu_H b_{SS}S_{SS}^{f***}}{\Pi_H} & 0 & \frac{\beta_V\mu_H b_{max}S_{SS}^{f***}}{\Pi_H}\\
0 & 0 & 0 & 0 & 0 & 0 & 0 & 0 & 0 & 0\\
0 & 0 & 0 & 0 & 0 & 0 & 0 & \frac{\beta_V\mu_H b_{RS}S_{RS}^{f***}}{\Pi_H} & 0 & \frac{\beta_V\mu_H b_{max}S_{RS}^{f***}}{\Pi_H}\\
0 & 0 & 0 & 0 & 0 & 0 & 0 & 0 & 0 & 0\\
0 & 0 & 0 & 0 & 0 & 0 & 0 & \frac{\beta_V\mu_H b_{RR}S_{RR}^{f***}}{\Pi_H} & 0 & \frac{\beta_V\mu_H b_{max}S_{RR}^{f***}}{\Pi_H}\\
0 & 0 & 0 & 0 & 0 & 0 & 0 & 0 & 0 & 0\\
0 & \beta_H b_{SS}C_B & 0 & \beta_H b_{RS}C_B & 0 & \beta_H b_{RR}C_B & 0 & 0 & 0 & 0\\
0 & 0 & 0 & 0 & 0 & 0 & 0 & 0 & 0 & 0\\
0 & \beta_H b_{max}(1-C_B) & 0 & \beta_H b_{max}(1-C_B) & 0 & \beta_H b_{max}(1-C_B) & 0 & 0 & 0 & 0\\
0 & 0 & 0 & 0 & 0 & 0 & 0 & 0 & 0 & 0
\end{bmatrix},$$

Box I.

and,

$$V=\begin{bmatrix}
K_{14} & 0 & 0 & 0 & 0 & 0 & 0 & 0 & 0 & 0\\
-\theta_{SS} & K_{13} & 0 & 0 & 0 & 0 & 0 & 0 & 0 & 0\\
0 & 0 & K_{16} & 0 & 0 & 0 & 0 & 0 & 0 & 0\\
0 & 0 & -\theta_{RS} & K_{15} & 0 & 0 & 0 & 0 & 0 & 0\\
0 & 0 & 0 & 0 & K_{18} & 0 & 0 & 0 & 0 & 0\\
0 & 0 & 0 & 0 & -\theta_{RR} & K_{17} & 0 & 0 & 0 & 0\\
0 & 0 & 0 & 0 & 0 & 0 & K_{19} & 0 & 0 & 0\\
0 & 0 & 0 & 0 & 0 & 0 & -\sigma_H & K_{20} & 0 & 0\\
0 & 0 & 0 & 0 & 0 & 0 & 0 & 0 & K_{19} & 0\\
0 & 0 & 0 & 0 & 0 & 0 & 0 & 0 & -\sigma_H & K_{20}
\end{bmatrix}.$$

The *reproduction number* of the model {(2.5)–(2.10)} (denoted by $\mathcal{R}_0$) is given by [53]:

$$\mathcal{R}_0=\rho(FV^{-1})=\sqrt{\frac{1}{2}\mathbb{R}_{HV}\left(\mathcal{R}_{0_1}+\sqrt{(\mathcal{R}_{0_1})^2+\mathcal{R}_{0_2}}\right)}\,, \tag{3.4}$$

where,

$$\mathbb{R}_{HV}=\frac{\beta_H\sigma_H}{K_{19}K_{20}},$$

$$\mathcal{R}_{0_1}=\beta_{SS}\mathbb{R}_{0_{SS}}+\beta_{RS}\mathbb{R}_{0_{RS}}+\beta_{RR}\mathbb{R}_{0_{RR}},$$

$$\mathcal{R}_{0_2}=4C_B(1-C_B)\left[\mathbb{R}_{0_{SS}}\mathbb{R}_{0_{RS}}(b_{SS}-b_{RS})^2+\mathbb{R}_{0_{SS}}\mathbb{R}_{0_{RR}}(b_{SS}-b_{RR})^2+\mathbb{R}_{0_{RR}}\mathbb{R}_{0_{RS}}(b_{RR}-b_{RS})^2\right],$$

with,

$$\beta_{SS}=C_Bb_{SS}^2+(1-C_B)b_{max}^2,\ \beta_{RS}=C_Bb_{RS}^2+(1-C_B)b_{max}^2,$$
$$\beta_{RR}=C_Bb_{RR}^2+(1-C_B)b_{max}^2,$$
$$\mathbb{R}_{0_{SS}}=\frac{\beta_V\theta_{SS}\mu_HS_{SS}^{f***}}{\Pi_HK_{13}K_{14}},\ \mathbb{R}_{0_{RS}}=\frac{\beta_V\theta_{RS}\mu_HS_{RS}^{f***}}{\Pi_HK_{15}K_{16}}\ \text{and}$$
$$\mathbb{R}_{0_{RR}}=\frac{\beta_V\theta_{RR}\mu_HS_{RR}^{f***}}{\Pi_HK_{17}K_{18}}.$$

The results below follows from Theorem 2 in [53].

Theorem 3.2. *Consider the model {(2.5)–(2.10)} with $0<p_i^{***},q_i^{***}<1$ $(i=f,m)$ and $\mathcal{R}_C>1$ (so that the non-trivial co-existence disease-free equilibrium ($\mathcal{T}_4$) exists). This equilibrium is locally-asymptotically stable if $\mathcal{R}_0<1$, and unstable if $\mathcal{R}_0>1$.*

The reproduction number $\mathcal{R}_0$ measures the average number of secondary infections generated by one infected human (mosquito of either of the three genotypes) introduced into a population of susceptible mosquitoes (humans) in a community where the aforementioned three insecticides-based interventions (larvicides, IRS and LLINs) are implemented [53]. The epidemiological implication of Theorem 3.2 is that, for the special case of the model {(2.5)–(2.10)} where the non-trivial co-existence disease-free equilibrium ($\mathcal{T}_4$) exists, a small influx of infected individuals (or mosquitoes) will not generate a large malaria outbreak in the community when the reproduction number of the model ($\mathcal{R}_0$) is less than unity. In other words, for the special case of the model where the non-trivial co-existence disease-free equilibrium exists, malaria can be effectively-controlled in the community if the initial sizes of the sub-populations of the model are in the basin of attraction of the non-trivial co-existence disease-free equilibrium ($\mathcal{T}_4$). For effective malaria control (or elimination) to be independent of initial sizes of the sub-populations of the model, a global asymptotic stability result must be established for this disease-free equilibrium. This is done in Section 3.2.2, for a special case of the model.

It is convenient to define the following genotype-specific threshold quantities:

$$\bar{\mathcal{R}}_{0_{SS}}=\sqrt{\mathbb{R}_{HV}\mathbb{R}_{0_{SS}}}\quad\text{and}\quad\bar{\mathcal{R}}_{0_{RR}}=\sqrt{\mathbb{R}_{HV}\mathbb{R}_{0_{RR}}}. \tag{3.5}$$

The quantity $\bar{\mathcal{R}}_{0_{SS}}$ ($\bar{\mathcal{R}}_{0_{RR}}$) is a constituent reproduction number of the model {(2.5)–(2.10)} which measures the average number of secondary infections generated by one infected human (mosquito of SS-genotype (RR-genotype)) introduced into a population of susceptible mosquitoes (humans) in a community with sensitive-only (resistant-only) mosquito population. Noting the definitions in (3.5), the following results (Theorem 3.3) can easily be recovered from the proof of Theorem 3.2.

Theorem 3.3. *Consider the model {(2.5)–(2.10)}.*

(i) If $\mathcal{R}_{SS}>1$, then the NTSDFE ($\mathcal{T}_2$) is locally-asymptotically stable if $\bar{\mathcal{R}}_{0_{SS}}<1$, and unstable if $\bar{\mathcal{R}}_{0_{SS}}>1$.

(ii) If $\mathcal{R}_{RR}>1$, then the NTRDFE ($\mathcal{T}_4$) is locally-asymptotically stable if $\bar{\mathcal{R}}_{0_{RR}}<1$, and unstable if $\bar{\mathcal{R}}_{0_{RR}}>1$.

3.2.2. Global asymptotic stability

The global asymptotic stability of the generalized non-trivial disease-free equilibrium ($\mathcal{T}_4$) will be explored for the special case of the model in the absence of disease-induced mortality in the human host population. That is, we will explore this result for the special case of the model {(2.5)–(2.10)} with $\delta_H=0$. It is convenient to define the threshold quantity $\mathcal{R}_{0C}=\mathcal{R}_0|_{\delta_H=0}$. We claim the following result:

Theorem 3.4. *Consider the special case of the model {(2.5)–(2.10)} with $\delta_H=0$. If $\mathcal{R}_C>1$ and $0<p_i^{***},q_i^{***}<1$ $(i=f,m)$ (so that the NTCDFE exists), then the non-trivial co-existence disease-free equilibrium ($\mathcal{T}_4$) is globally-asymptotically stable in $\Omega\setminus(\mathcal{T}_1\cup\mathcal{T}_2\cup\mathcal{T}_3)$ whenever $\mathcal{R}_{0C}<1$.*

Proof. The proof of Theorem 3.4, based on using a comparison theorem, is given in the Appendix. □

The epidemiological implication of Theorem 3.4 is that, for the special case of the model {(2.5)–(2.10)} with $\delta_H = 0$ (and conditions for the existence of the non-trivial co-existence disease-free equilibrium, $\mathcal{T}_4$, are met), bringing (and maintaining) the reproduction number $\mathcal{R}_{0C}$ to a value less than unity is necessary and sufficient for the effective control (or elimination) of malaria from the community. In other words, the insecticides-based control strategies adopted in the community (i.e., larvicides, IRS and LLINs) can lead to the effective control or elimination of malaria if they can reduce (and maintain) the reproduction number $\mathcal{R}_{0C}$ to a value less than unity. The following results can also be recovered from the proof of Theorem 3.4:

Theorem 3.5. *Consider the special case of the model {(2.5)–(2.10)} with $\delta_H = 0$.*

(i) If $\mathcal{R}_{SS} > 1$, then the NTSDFE ($\mathcal{T}_2$) is globally-asymptotically stable in $\Omega \setminus (\mathcal{T}_1 \cup \mathcal{T}_3 \cup \mathcal{T}_4)$ whenever $\bar{\mathcal{R}}_{0_{SS}} < 1$.

(ii) If $\mathcal{R}_{RR} > 1$, then the NTRDFE ($\mathcal{T}_3$) is globally-asymptotically stable in $\Omega \setminus (\mathcal{T}_1 \cup \mathcal{T}_2 \cup \mathcal{T}_4)$ whenever $\bar{\mathcal{R}}_{0_{RR}} < 1$.

4. Numerical simulations

In this section, numerical simulations of the developed model {(2.5)–(2.10)} will be carried out to primarily quantify the extent and impact of the interactions of the three insecticide-based anti-malaria control strategies (larvicide, LLINs and IRS) on disease control and resistance management. Simulations will also be carried out to assess the impact of the parameter governing the number of new adult mosquitoes that are females (r) and the initial frequency of resistant allele in the community. The simulations will be carried out using data from the Asendabo Health Center of the Jimma Zone in Southwestern Ethiopia. The health center serves an estimated population of 49,817, and Jimma Zone is considered to be an area of high malaria transmission (with estimated malaria prevalence of about 32.4%) [22,54].

4.1. Parameters and initial conditions

4.1.1. Human demographic parameters and initial conditions

Based on the data for Jimma Zone presented by Demissie et al. [54], the following initial values for the number of humans in the various epidemiological compartments of the model (i.e., the sum of both the LLINs-protected and LLINs-unprotected individuals in each epidemiological compartment) are chosen (it should be stated that we split the total malaria-infected human population into 12% exposed and 20.4% infectious):

$$S_H(0) = 23,916,\ E_H(0) = 5,977,\ I_H(0) = 9,964 \text{ and } R_H(0) = 9,962.$$

Thus, when an LLINs intervention program is implemented in the community (at a coverage level C_B), the initial values for the number of humans in the various epidemiological compartments become:

$$\begin{aligned} S_{H_p}(0) &= C_B S_H(0), E_{H_p}(0) = C_B E_H(0), I_{H_p}(0) = C_B I_H(0),\\ R_{H_p}(0) &= C_B R_H(0),\\ S_{H_u}(0) &= (1-C_B) S_H(0), E_{H_u}(0) = (1-C_B) E_H(0),\\ I_{H_u}(0) &= (1-C_B) I_H(0),\\ R_{H_u}(0) &= (1-C_B) R_H(0). \end{aligned}$$

Following Mohammed-Awel and Gumel [22], the human recruitment rate parameter (Π_H) is estimated based on the above mentioned total population size of the Jimma zone and the average human lifespan in Ethiopia (65 years), and is set at 2.19 *per* day. The value of the maximum adult mosquito biting rate b_{max} is set at 2 bites *per* day for this transmission setting [22]. Other parameter values chosen for the simulations of the model are as given in Tables 2–4 (unless otherwise stated).

4.1.2. Initial distribution of mosquitoes by genotype

The initial mosquito population to be used in the numerical simulations of the model is stratified based on the level of the frequency of resistant allele ($p_f(0)$ and $p_m(0)$ for female and male mosquitoes, respectively) in the malaria-endemic community. We consider the following three levels of frequency of the resistant allele in the community:

Low level of frequency of resistant allele: for this level, we assume 10% of the mosquitoes carry the resistant allele, while the remaining 90% carry the sensitive allele. It should be recalled that the allele frequency for immature (adult) mosquitoes is calculated by adding the total number of immature (adult) homozygous resistant mosquitoes to half the total number of immature (adult) heterozygous resistant mosquitoes and the result divided by the total number of immature (adult) mosquitoes in the community. To achieve the low level allele frequency in the mosquito population (with 10% of mosquitoes carrying the resistant allele (i.e., $p_f(0) = p_m(0) = 0.1$), and the remaining 90% carrying the sensitive allele (i.e., $q_f(0) = q_m(0) = 0.9$)), the following initial values (with female:male sex ratio 52:48) for the various mosquito (immature and adult) populations (by genotype) are chosen:

$$\begin{aligned} E_{SS}(0) &= 866,667, E_{RS}(0) = 66,666, E_{RR}(0) = 66,667,\\ L_{SS}(0) &= 734,933, L_{RS}(0) = 56,534,\\ L_{RR}(0) &= 56,533, P_{SS}(0) = 624,000, P_{RS}(0) = 48,000, P_{RR}(0) = 48,000,\\ M_{SS}(0) &= 60,667,\\ M_{RS}(0) &= 4,666, M_{RR}(0) = 4,667, S^f_{SS}(0) = 43,333, E^f_{SS}(0) = 3,334,\\ I^f_{SS}(0) &= 3,333,\\ S^f_{RS}(0) &= 9,167, E^f_{RS}(0) = 1,666, I^f_{RS}(0) = 1,667, S^f_{RR}(0) = 9,167,\\ E^f_{RR}(0) &= 1,666,\\ I^f_{RR}(0) &= 1,667. \end{aligned} \tag{4.1}$$

Moderate level of frequency of resistant allele: here, following the report in [22,29], we consider 37.5% of the local mosquitoes to carry the resistant allele (i.e., $p_f(0) = p_m(0) = 0.375$), while the remaining 62.5% carry the sensitive allele (i.e., $q_f(0) = q_m(0) = 0.625$). In this case, the following initial values (with female:male sex ratio 59:41) for the various mosquito populations (by genotype) are chosen:

$$\begin{aligned} E_{SS}(0) &= 500,000, E_{RS}(0) = 250,000, E_{RR}(0) = 250,000,\\ L_{SS}(0) &= 424,000, L_{RS}(0) = 212,000,\\ L_{RR}(0) &= 212,000, P_{SS}(0) = 360,000, P_{RS}(0) = 180,000,\\ P_{RR}(0) &= 180,000, M_{SS}(0) = 35,000,\\ M_{RS}(0) &= 17,500, M_{RR}(0) = 17,500, S^f_{SS}(0) = 25,000, E^f_{SS}(0) = 12,500,\\ I^f_{SS}(0) &= 12,500,\\ S^f_{RS}(0) &= 12,500, E^f_{RS}(0) = 6,250, I^f_{RS}(0) = 6,250, S^f_{RR}(0) = 12,500,\\ E^f_{RR}(0) &= 6,250,\\ I^f_{RR}(0) &= 6,250. \end{aligned} \tag{4.2}$$

High level of frequency of resistant allele: here, we consider 80% of the mosquitoes to carry the resistant allele (i.e., $p_f(0) = p_m(0) = 0.8$), while the remaining 20% carry the sensitive allele (i.e., $q_f(0) = q_m(0) = 0.2$). Here, the following initial distribution (with female:male sex ratio 59:41) of the mosquito population (by genotype) is chosen:

$$\begin{aligned} E_{SS}(0) &= 100,000, E_{RS}(0) = 200,000, E_{RR}(0) = 700,000,\\ L_{SS}(0) &= 84,800, L_{RS}(0) = 169,600,\\ L_{RR}(0) &= 593,600, P_{SS}(0) = 72,000, P_{RS}(0) = 144,000,\\ P_{RR}(0) &= 504,000, M_{SS}(0) = 7,000,\\ M_{RS}(0) &= 14,000, M_{RR}(0) = 49,000, S^f_{SS}(0) = 10,000, E^f_{SS}(0) = 2,500,\\ I^f_{SS}(0) &= 2,500, \end{aligned} \tag{4.3}$$

$S^f_{RS}(0) = 5,000, E^f_{RS}(0) = 2,500, I^f_{RS}(0) = 2,500, S^f_{RR}(0) = 50,000,$
$E^f_{RR}(0) = 12,500,$
$I^f_{RR}(0) = 12,500.$

4.2. Simulations: Worst-case scenario

The model {(2.5)–(2.10)} is, first of all, simulated for the worst-case scenario (i.e., without any anti-malaria control interventions, so that $C_B = C_A = C_L = 0$) using the parameter values in Tables 2–4 and initial conditions for the human and vector populations corresponding to the aforementioned moderate level of the frequency of resistant allele in the community. The profiles generated from the simulations show convergence of the initial solutions to a boundary equilibrium involving only the sensitive adult mosquitoes (Fig. 2). In other words, the results in this figure show that, for the parameter values used in the simulations, the resistant adult mosquito population (both heterozygous and homozygous resistant) will not persist in the Jimma zone even if no insecticide-based mosquito control measures are implemented. This may be due to the high fitness cost of insecticide resistance and the low level of dominance of the resistance allele ($h = 0.25$) used in the simulations (tabulated in Tables 2–4).

For the rest of the numerical simulations to be carried out, the following definitions will be used. We consider the disease to be *effectively controlled* if the associated steady-state prevalence of the disease in the human population is less than 1%. The justification for using the 1% criterion for claiming effective control of malaria in the community stemmed from the World Health Organization's criterion for issuing "certification of malaria elimination" to nations/countries that achieved malaria elimination. The criterion for getting this certification is based on whether or not a specific nation or country achieves at least three consecutive years of zero indigenous cases of malaria [55]. For nations with high malaria transmission, coupled with limited healthcare services and resources (to effective implement mosquito control strategies), such as the Jimma Zone of Southwestern Ethiopia (where this study is focused on), bringing prevalence down to 1% is a laudable achievement, and can plausibly be considered to be "effective control" of malaria. Furthermore, we consider insecticide resistance (i.e., the proportion or frequency of the resistant allele in the adult female and male mosquito populations at steady-state) to be *effectively managed* if the frequency of the resistant allele in the adult mosquito population at steady-state is zero. That is, insecticide resistance is effectively managed in the community if, at steady-state, the adult mosquito population is 100% fully sensitive to the chemical insecticides used in larvicides, LLINs and IRS (i.e., all adult mosquitoes in the community are of SS-genotype only at steady-state).

4.3. Assessing the additional population-level impact of larvicide intervention in the presence of LLINs and IRS

The model {(2.5)–(2.10)} is simulated to assess the additional population-level impact of implementing a larvicide-based control measure in a community that is already implementing LLINs and IRS mosquito control measures. The motivation is to determine what minimum levels (if any) of the three interventions can lead to the effective control of malaria, while effectively managing insecticide resistance. For these simulations, various fixed values of larvicide coverage (C_L) are used, while allowing IRS (C_A) and bednets (C_B) coverage to vary between 0% and 100%. Other parameter values used in these simulations are as given in Tables 2–4 with moderate initial resistant allele frequency of $p_f(0) = p_m(0) = 37.5\%$. Three values of larvicide coverage are considered as discussed below.

4.3.1. No larvicide coverage ($C_L = 0$)

In the absence of larviciding (i.e., $C_L = 0$), the simulation results obtained show that LLINs are far more effective in minimizing malaria burden than using IRS (Fig. 3(a)). In particular, the simulations show that LLINs alone (i.e., without IRS and larviciding) can lead to the effective control (or elimination) of malaria, while also effectively managing insecticide resistance, if its coverage level is high enough (e.g., $C_B \geq 0.9$) (Fig. 3(a)–(d)). Attaining 90% LLINs coverage is certainly not realistic in pretty much all the malaria-endemic areas of the world (in fact, data from the 2019 World Malaria Report published by the World Health Organization [4] show that LLINs coverage in populations at risk lie between 40% and 80%). Consequently, simulations are carried out to explore whether or not LLINs at reduced (attainable) coverage can lead to such control if it is combined with IRS (in the presence or absence of larviciding). The simulations results obtained for this (latter) scenario, depicted in Fig. 3(a), show that a combined LLINs-IRS strategy can lead to the effective control of malaria if their coverage lie within the region below the straight line joining the points $(C_B, C_A) = (0.75, 0.32)$ and $(C_B, C_A) = (1, 0.22)$, and above the straight line joining the points $(C_B, C_A) = (0.75, 0.32)$ and $(C_B, C_A) = (0.9, 0)$. This region in the LLINs-IRS coverage parameter space (for the effective control of malaria, while also effectively managing insecticide resistance) is termed an *effective control window*. Although the disease is not effectively controlled outside this effective control window, its prevalence is low (less than 5%) when the LLINs-IRS coverage pair is close to the borders of this region. Furthermore, for these simulations, insecticide resistance is effectively managed provided that the LLINs-IRS coverage pair lie roughly in the region below the straight line joining the points $(C_B, C_A) = (0, 0.72)$ and $(C_B, C_A) = (1, 0.23)$ (Fig. 3(b) & (c)). Outside this region, insecticide resistance is not effectively managed. Additionally, the disease is effectively controlled and insecticide resistance effectively managed for LLINs-IRS coverage in the intersection of the aforementioned two regions.

Assuming the best case scenario of 80% LLINs coverage suggested in the WHO data [4] (i.e., $C_B = 0.8$), our simulation results show that combining LLINs (at this highly optimistic coverage level) with moderate IRS coverage (e.g., $C_A \in (0.11, 0.3225)$) can lead to effective control of malaria, while also effectively managing insecticide resistance (Fig. 3(a)–(c)). However, if this level of bednets coverage is combined with an IRS program at a coverage level outside the $C_A \in (0.11, 0.3225)$ range, the aforementioned effective control of the disease no longer holds, and insecticide resistance is not effectively managed if the IRS coverage exceeds $C_A = 0.3225$. This is due to the fact that such an increase in IRS usage (above $C_A = 0.3225$) contributes to significant increase in the prevalence of the resistant allele in the population, and a decrease in IRS usage (below $C_A = 0.11$) is not sufficient to protect humans from receiving infectious bites from infected female *Anopheles* mosquitoes (Fig. 3(b) & (c)). This fact can be illustrated by using the respective constituent reproduction numbers for the SS-genotype ($\mathcal{R}_{0_{SS}}$) and RR-genotype ($\mathcal{R}_{0_{RR}}$) mosquitoes. For example, for the case where $C_A = 0.3225$ and $C_B = 0.8$, the genotype-specific reproduction numbers $\mathcal{R}_{0_{RR}}$ and $\mathcal{R}_{0_{SS}}$ take the values $\mathcal{R}_{0_{RR}} = 0$ and $\bar{\mathcal{R}}_{0_{SS}} = \mathcal{R}_0 = 0.4792$, respectively (and the solution profiles of the model converge to the trivial mosquito-free disease-free equilibrium, $\mathcal{T}_1$, as expected). If the IRS coverage is, however, slightly increased to, for instance, $C_A = 0.323$, these values now become $\bar{\mathcal{R}}_{0_{RR}} = \mathcal{R}_0 = 7.1968$ and $\bar{\mathcal{R}}_{0_{SS}} = 0$ (and the solutions of the model converge to a positive boundary equilibrium with the resistant-only mosquitoes present in the community). Thus, the slight increase in the IRS coverage resulted in a dramatic increase in the transmission capacity of the insecticide-resistant malaria-infected adult female mosquitoes (from $\bar{\mathcal{R}}_{0_{RR}} = 0$ to $\mathcal{R}_{0_{RR}} = 7.1968$), causing disease endemicity (as against elimination in the former case) and the sole persistence of the mosquitoes with the resistant genotype in the community (i.e., the sensitive mosquitoes are wiped out under this scenario).

Similarly, for the case when $C_A = 0.11$ and $C_B = 0.8$, the constituent reproduction numbers take the values $\bar{\mathcal{R}}_{0_{SS}} = \mathcal{R}_0 = 0.9902 < 1$ and $\mathcal{R}_{0_{RR}} = 0$ (and the solutions of the model converge to the mosquito-free trivial disease-free equilibrium). A slight decrease in IRS coverage

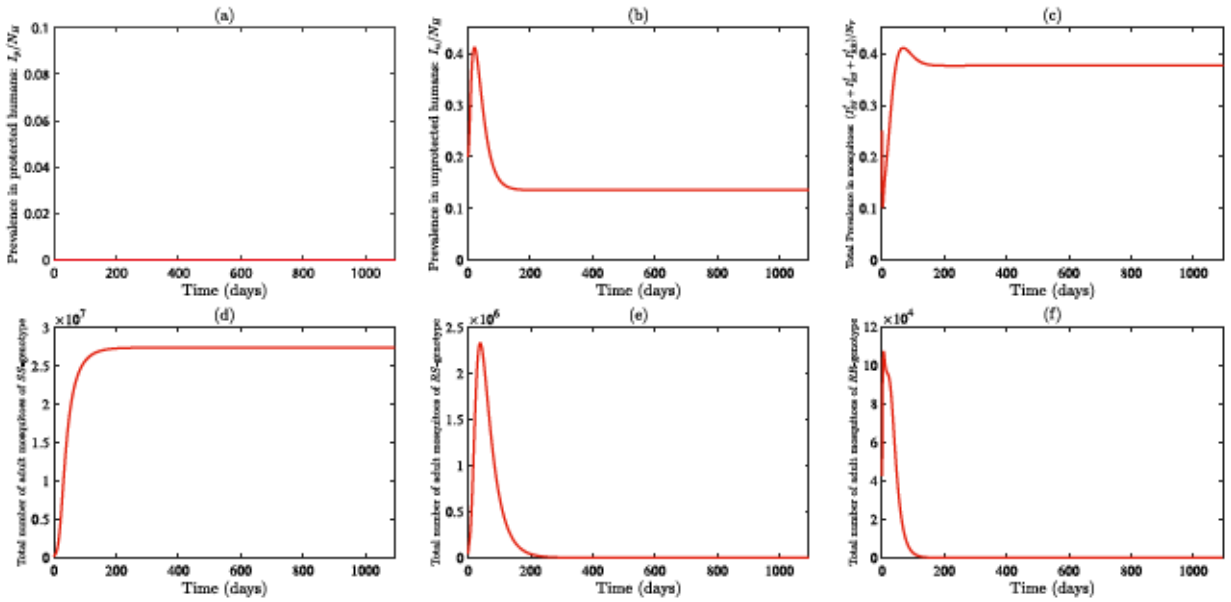

Fig. 2. Simulations of the model system {(2.5)–(2.10)} for worst-case scenario, showing (a) malaria prevalence in protected humans (I_p/N_H), (b) malaria prevalence in unprotected humans (I_u/N_H), (c) total malaria prevalence in adult female mosquitoes ($(I^f_{SS}+I^f_{RS}+I^f_{RR})/N^f_V$, where $N^f_V = S^f_{SS}+E^f_{SS}+I^f_{SS}+S^f_{RS}+E^f_{RS}+I^f_{RS}+S^f_{RR}+E^f_{RR}+I^f_{RR}$), (d) total number of adult mosquitoes of SS-genotype, (e) total number of adult mosquitoes of RS-genotype, and (f) total number of adult mosquitoes of RR-genotype. The parameter values chosen are the same as the baseline values given in Tables 2–4, with $C_B = C_A = C_L = 0$ and with moderate initial resistant allele frequency given in (4.2). For this setting, the basic reproduction number associated with the non-trivial sensitive-only disease-free equilibrium ($\bar{\mathcal{R}}_{0_{ss}}$) takes the value $\bar{\mathcal{R}}_{0_{ss}} = 111.83 > 1$. Similarly, the threshold quantity for the persistence of the SS-genotype mosquitoes ($\mathcal{R}_{SS}$) takes the value $\mathcal{R}_{SS} = 13.68 > 1$.

from $C_A = 0.11$ to $C_A = 0.1$ results in these values changing to $\mathcal{R}_{0_{SS}} = \mathcal{R}_0 = 1.0184$ and $\mathcal{R}_{0_{RR}} = 0$. Hence, in this latter case, the slight reduction in IRS coverage resulted in correspondingly slight increase in the constituent reproduction number for the sensitive mosquitoes. Although this increase in $\bar{\mathcal{R}}_{0_{SS}}$ is marginal (from $\bar{\mathcal{R}}_{0_{SS}} = 0.9902$ to $\mathcal{R}_{0_{SS}} = 1.0184$, it is significant in the sense that it shifts the value of the reproduction number from the disease-free region (i.e., $\bar{\mathcal{R}}_{0_{SS}} < 1$) to an endemic one (i.e., $\mathcal{R}_{0_{SS}} > 1$)). Here, the solutions of the model converged to a positive boundary equilibrium involving insecticide-sensitive mosquitoes only (i.e., in this case, the slight reduction in the IRS coverage resulted in a change in the genotype of the mosquito that is present at the boundary disease-present equilibrium).

Furthermore, because of random mating, the size of the death rate of the RS-genotype mosquitoes determines whether the system converges to the one of the boundary (SS-only or RR-only) equilibria, the co-existence or mosquito-free equilibrium. For example, if the size of the S-allele frequency is much smaller than that of the R-allele frequency in the population, and the death rate of the RS-genotype is high, then the model will converge to RR-only equilibrium. Due to this phenomenon, if the (C_A, C_B) value is close to the boundary between the effective control window and the region outside the window in the C_A–C_B plane, then the genotype-specific reproduction numbers are sensitive to small changes in h (since h affects the size of the death rate of RS-genotype). For example, fixing C_A at the value $C_A = 0.323$ (in Fig. 3(a)) (with this value, the system will converge to the RR-only boundary equilibrium), a small decrease in h (e.g., a decrease from $h = 0.25$ to $h = 0.247$) changes the genotype-specific reproduction numbers to $\mathcal{R}_{0_{RR}} = \mathcal{R}_0 = 0$ and $\bar{\mathcal{R}}_{0_{SS}} = 0.4780$ (and the solutions of the model converge to the SS-only boundary equilibrium). Thus, for (C_A, C_B) values on the boundary of the effective control window, the basic reproduction thresholds are sensitive to small changes in the values of C_A, C_B and h. The effect of the level of dominance h is further discussed in Section 4.6.

In summary, the simulations for the case with no larvicide ($C_L = 0$) show that LLINs alone, at high coverage, can lead to the effective control of malaria while effectively managing insecticide resistance. However, the required LLINs coverage (of over 90%) may not be realistically-attainable in malaria-endemic settings (the maximum LLINs coverage reported in the 2019 World Malaria Report is 80% [56]). Combining LLINs and IRS can also lead to the effective control of malaria while managing insecticide resistance provided the coverage levels of both interventions lie within a certain threshold. For instance, for the (highly) optimistic scenario of 80% LLINs coverage, effective control of malaria and effective management of resistance is only feasible if the IRS coverage lie roughly within 11% to 32%. Furthermore, the simulations show that there exists an *effective control window* in the LLINs-IRS coverage parameter space within which both the disease and insecticide resistance can be effectively managed. Starting with the coverage levels of LLINs and IRS within the effective control window, it is evident from Fig. 3(a)–(c) that any further increase in IRS coverage (above its range of values within the effective control window) will lead to the failure of the combined LLINs-IRS strategy to effectively manage both disease spread and insecticide resistance (since such increase in IRS coverage will take the community outside the effective control window). The reason for this failure is due to the fact that IRS affects both sexes of the malaria vector, causing high selection pressure for insecticide resistance (leading to the overall failure of the control strategy). It should be noted that LLINs induce less selection pressure for resistance, since, unlike IRS and larviciding, it only targets adult female mosquitoes (and not male mosquitoes). This fact was also elucidated in [16].

4.3.2. *Low larvicide coverage ($C_L = 0.1$)*

The model is now simulated using a low larvicide coverage of 10% (i.e., $C_L = 0.1$). The simulation results obtained (depicted in Fig. 3(d)–(f)) also show that LLINs alone (i.e., without IRS) can lead to the effective control of malaria while effectively managing insecticide resistance as long as its coverage level is high enough (e.g., $C_B \geq 0.85$). Further, these figures show that such effective control and resistant management are feasible if the combined LLINs-IRS coverage lies in the narrow region enclosed by the quadrilateral with the vertices $(C_B, C_A) = (0.75, 0)$, $(C_B, C_A) = (0.85, 0)$, $(C_B, C_A) = (0.8, 0.057)$ and $(C_B, C_A) = (0.7, 0.057)$ or LLINs-only with coverage in the range $0.85 \leq C_B \leq 1$ (Fig. 3(d)). Here, too, although the disease is not effectively

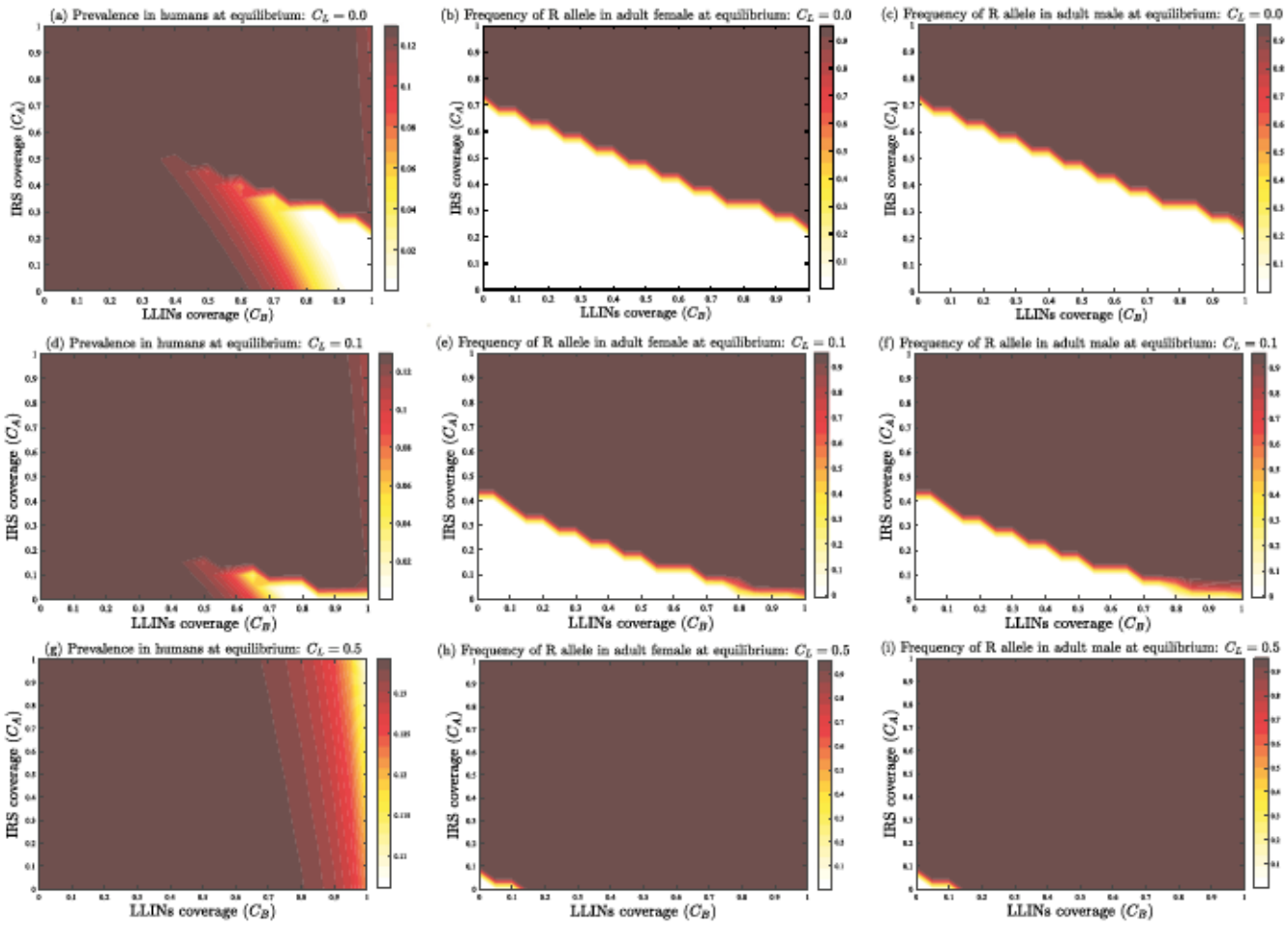

Fig. 3. Heat map of the model {(2.5)–(2.10)} for bednets (LLINs) coverage (C_B) *vs.* IRS coverage (C_A). Parameter values are as given by the baseline values in Tables 2–4, and with the moderate initial resistant allele frequency given in (4.2). (i). (a)–(c) $C_L = 0$, (ii) (d)–(f) $C_L = 0.1$, and (iii) (g)–(i) $C_L = 0.5$.

controlled for the LLINs-IRS coverage pairs outside this region, the disease prevalence is low (less than 5%) when the LLINs-IRS coverage pair is close to the borders of this region. For the (highly) optimistic LLINs coverage of 80% [4], the simulation results obtained show that LLINs alone (at this coverage level) or combined with IRS (at coverage range $0 \leq C_A \leq 0.057$) can lead to effective control of malaria while effectively managing insecticide resistance (Fig. 3(d)–(f)). However, if this level of LLINs coverage is combined with IRS coverage outside the $0 \leq C_A \leq 0.057$ range, the disease is not effectively controlled and insecticide resistance is not effectively managed. This can be seen from the values of the reproduction numbers. For the case when $C_A = 0.057$ and $C_B = 0.8$, the reproduction numbers for the SS-genotype and RR-genotype adult mosquitoes take the value zero (and the profiles generated from the simulations show convergence of the initial solutions to the ecologically-unrealistic mosquito-free trivial disease-free equilibrium). However, when the IRS coverage is slightly increased to $C_A = 0.058$, the constituent reproduction numbers take the values $\mathcal{R}_{0_{SS}} = 0.1471$ and $\mathcal{R}_{0_{RR}} = 6.7197$ (so that $\mathcal{R}_0 = 10.0132$). Thus, such slight increase in IRS coverage resulted in a dramatic increase in the transmission capacity of the resistant mosquitoes (here, the solution profiles of the model converged to an endemic equilibrium where both mosquito genotypes co-exist).

In summary, these simulations show that the marginal increase in larviciding coverage (from $C_L = 0$ to $C_L = 0.1\%$) narrows the effective window of the LLINs-IRS coverage needed to effectively control malaria while effectively managing insecticide resistance. In other words, the slight increase in larvicide coverage reduces the likelihood of effective disease control and enhances the prospects of insecticide resistance in the community. These simulations also show that starting with LLINs and IRS coverage pairs within the effective control window, any further increases in the coverage level of IRS (above its range within the effective control window) will lead to the failure of the control (to combat malaria spread and to manage resistance) Fig. 3(d)–(f). Similarly, as shown in Fig. 3(a), (d) and (g), increases in larviciding coverage result in significant shrinkage of the effective control window (thereby causing the aforementioned failure of the insecticides-based intervention).

4.3.3. *Moderate larvicide coverage ($C_L = 0.5$)*

For the case when larvicide coverage is increased to the moderate level of $C_L = 0.5$, the simulation results obtained (Fig. 3(g)–(i)) show that effective control of malaria is not feasible regardless of the coverage levels of both LLINs and IRS. This result may sound counter-intuitive, since, ordinarily, more control (i.e., more larvicides, LLINs and IRS) should imply reduction of disease burden. However, increasing the coverages of these controls intuitively increases the abundance of the resistant mosquitoes; hence, an increase in the number of malaria cases caused by the resistant mosquitoes. The simulations in Fig. 3(g)–(i)) also show that insecticide resistance is not effectively managed for all LLINs-IRS coverage levels except for the coverage pair lying in the small white region at the left bottom corner of the C_B–C_A plane in Fig. 3(g).

In conclusion, the simulations in Fig. 3 show that there is a region in the C_B–C_A plane in which the community-wide use of LLINs and IRS can lead to the effective control of malaria and effective management of insecticide resistance. The size of this region is greatly reduced (or diminished altogether or vanished) as the coverage level of larviciding (C_L) increases. Furthermore, starting with the coverage levels of LLINs and IRS within the effective control window, an increase in IRS coverage (outside its range of values within the effective control window) will lead to the failure of the insecticides-based intervention (Fig. 3).

4.4. Assessing the population-level effect of adult mosquito sex ratio (r)

In most modeling studies for population genetics of mosquitoes, the simplifying assumption of 50:50 male:female ratio for new adult mosquitoes is often made [57,58]. In this section, the impact of heterogeneity in the proportion of new adult mosquitoes (as represented by the parameter r in our model) on the population abundance of mosquitoes and malaria disease will be assessed, under various levels of mosquito control interventions. In particular, the model will be simulated using various values of r for two coverage levels of larviciding ($C_L = 0$ and $C_L = 0.1$) and variable coverage levels for LLINs and IRS, as described below.

4.4.1. Low proportion of new adult mosquitoes that are females ($r = 0.35$) and no larvicide coverage ($C_L = 0$)

The model is first of all simulated for the case where the proportion of new adult mosquitoes that are females is low ($r = 0.35$) in the absence of larviciding ($C_L = 0$). The simulation results obtained show that LLINs alone (i.e., without larvicides and IRS) can lead to the effective control of malaria if its coverage is at least 77% (Fig. 4(a)). Furthermore, for this setting, the use of LLINs as the sole anti-malaria intervention, regardless of its coverage level, effectively manages insecticide resistance (Fig. 4(b) & (c)). It is evident from these figures that this result also holds even if LLINs is combined with IRS at low coverage level (e.g., IRS coverage in the range $0 \leq C_A \leq 0.27$). Additionally, the disease is effectively controlled if the LLINs-IRS coverage pair fall roughly within the region below the straight line joining the points $(C_B, C_A) = (0.45, 0.4)$ and $(C_B, C_A) = (1, 0.22)$, and above the straight line joining the points $(C_B, C_A) = (0.45, 0.4)$ and $(C_B, C_A) = (0.75, 0)$ (Fig. 4(a)). The disease is not effectively controlled outside this region (*albeit* the disease prevalence is low if the LLINs-IRS coverage is close to the border of this region). Insecticide resistance is effectively managed provided that the LLINs-IRS coverage lie in the region below the straight line connecting the points $(C_B, C_A) = (0, 0.65)$ and $(C_B, C_A) = (1, 0.15)$ (Fig. 4(b) & (c)). Insecticide resistance is not effectively managed outside this region.

It is worth mentioning that, in this setting, LLINs with low coverage (up to $C_B = 0.45$) can lead to the effective control of the disease, while also effectively managing insecticide resistance, if combined with IRS at appropriate coverage level. For example, combining LLINs at the 45% coverage level with IRS at 40% coverage level leads to the aforementioned disease control and resistance management (Fig. 4(a), (b), (c)). It should be recalled from Fig. 3(a) that, for the $(C_B, C_A) = (0.45, 0.4)$ coverage pair, such disease control does not occur if the proportion of new adult mosquitoes that are females is increased to 50% (i.e., the combined LLINs-IRS intervention at this moderate coverage levels does not lead to effective disease control if half of the newly-produced adult mosquitoes are females). In conclusion, for the case where the proportion of new adult mosquitoes that are females is small (e.g., $r = 0.35$), LLINs alone can lead to the effective control of malaria while effectively managing insecticide resistance provided the LLINs coverage is high enough (at least 77%). Further, such effective control and resistance management are also feasible using a combined LLINs-IRS strategy with moderate coverage levels (e.g., LLINs at 45% combined with IRS at 40% coverage level). Such control and resistance management does not occur (at the aforementioned LLINs and IRS coverage levels) if the proportion of new adult mosquitoes that are females is increased from 35% to 50% (as can be seen by comparing Figs. 3(a) & 4(a)).

4.4.2. High proportion of new adult mosquitoes that are females ($r = 0.65$) and no larvicide coverage ($C_L = 0$)

Here, the model is simulated for the case where the proportion of new adult mosquitoes that are females is increased to 65% (i.e., $r = 0.65$) while keeping larvicide at zero coverage. The simulation results obtained, depicted in Fig. 4(d)), show that LLINs alone can also lead to the effective control of the disease if its coverage level is high enough (at least 95%). The window for the effective control of the disease significantly narrows, in comparison to the case with $r = 0.35$ (see Figs. 3(a) and 4(a)). In other words, these simulations show that increasing the ratio of new adult mosquitoes that are females (from 35% to 65%) makes it more difficult to effectively control malaria disease, as expected. Furthermore, it follows from Fig. 4(a) that LLINs even if combined with IRS (but at low IRS coverage, such as $0 \leq C_A \leq 0.28$) effectively manages insecticide resistance (Fig. 4(e) & (f)). Furthermore, Fig. 4(d) shows that the combined LLINs-IRS intervention can lead to the effective management of the disease if the LLINs-IRS coverage lies in the region below the straight line joining the points $(C_B, C_A) = (0.85, 0.3)$ and $(C_B, C_A) = (1, 0.25)$, and above the straight line joining the points $(C_B, C_A) = (0.85, 0.3)$ and $(C_B, C_A) = (0.75, 0)$. The disease is not controlled outside this region (although the disease prevalence is low if the LLINs-IRS coverage is close to the border of this region). Similarly, insecticide resistance is effectively managed provided that the LLINs-IRS coverage lies in the region below the straight line connecting the points $(C_B, C_A) = (0, 0.72)$ and $(C_B, C_A) = (1, 0.15)$ (Fig. 4(b) & (c)). It is worth noting that the region for the effective control of disease, while effectively managing insecticide resistance, for the case with $r = 0.65$ is narrower than the corresponding regions for the cases where $r = 0.35$ and $r = 0.5$ (see Figs. 3(a) & 4(a) & (d)). This emphasizes the fact that the larger the proportion of new adult mosquitoes that are females, the more difficult (expectedly) it is to effectively control the disease and manage insecticide resistance.

4.4.3. Low proportion of new adult mosquitoes that are females ($r = 0.35$) and low larvicide coverage ($C_L = 0.1$)

The model is now simulated for the case where larvicide coverage is slightly increased to 10% (i.e., $C_L = 0.1$). For the case when $r = 0.35$, the results obtained show that LLINs alone can lead to the effective control of the disease provided its coverage lie in the range $0.53 \leq C_B \leq 1$ (Fig. 4(g)). Furthermore, LLINs alone (with level of coverage in the range $0 \leq C_B \leq 0.6$) effectively manages insecticide resistance (Fig. 4(h) & (i)). Fig. 4(g) further shows that malaria is effectively controlled if the coverage of the combined LLINs-IRS program lies in the region below the straight line joining the points $(C_B, C_A) = (0.35, 0.2)$ and $(C_B, C_A) = (0.75, 0)$, and above the straight line joining the points $(C_B, C_A) = (0.35, 0.2)$ and $(C_B, C_A) = (0.5, 0)$. In this setting, insecticide resistance is effectively managed provided that the coverage of the LLINs-IRS program lies in the region below the straight line connecting the points $(C_B, C_A) = (0, 0.4)$ and $(C_B, C_A) = (0.6, 0)$ (Fig. 4(h) & i)). In summary, the simulations of the model for the case with $C_L = 0.1$ and $r = 0.35$ show that the slight increase in larvicide coverage (from 0 to 10%) resulted in the narrowing of the effective control window (in the C_B–C_A plane) for the effective control of malaria, in addition to also significantly raising the likelihood of insecticide resistance. Similar results were obtained when r was increased to 65%. Thus, it can be concluded from these simulations that there is a region in the C_B–C_A plane within which the combined LLINs-IRS intervention can lead to the effective control of the disease, while also effectively managing insecticide resistance. The size of this region decreases with increasing values of larvicide coverage (C_L) and the proportion of new adult mosquitoes that are females (r). It is worth mentioning that, for the case where $C_L = 0.1$ and $r = 0.65$, while LLINs alone (with coverage

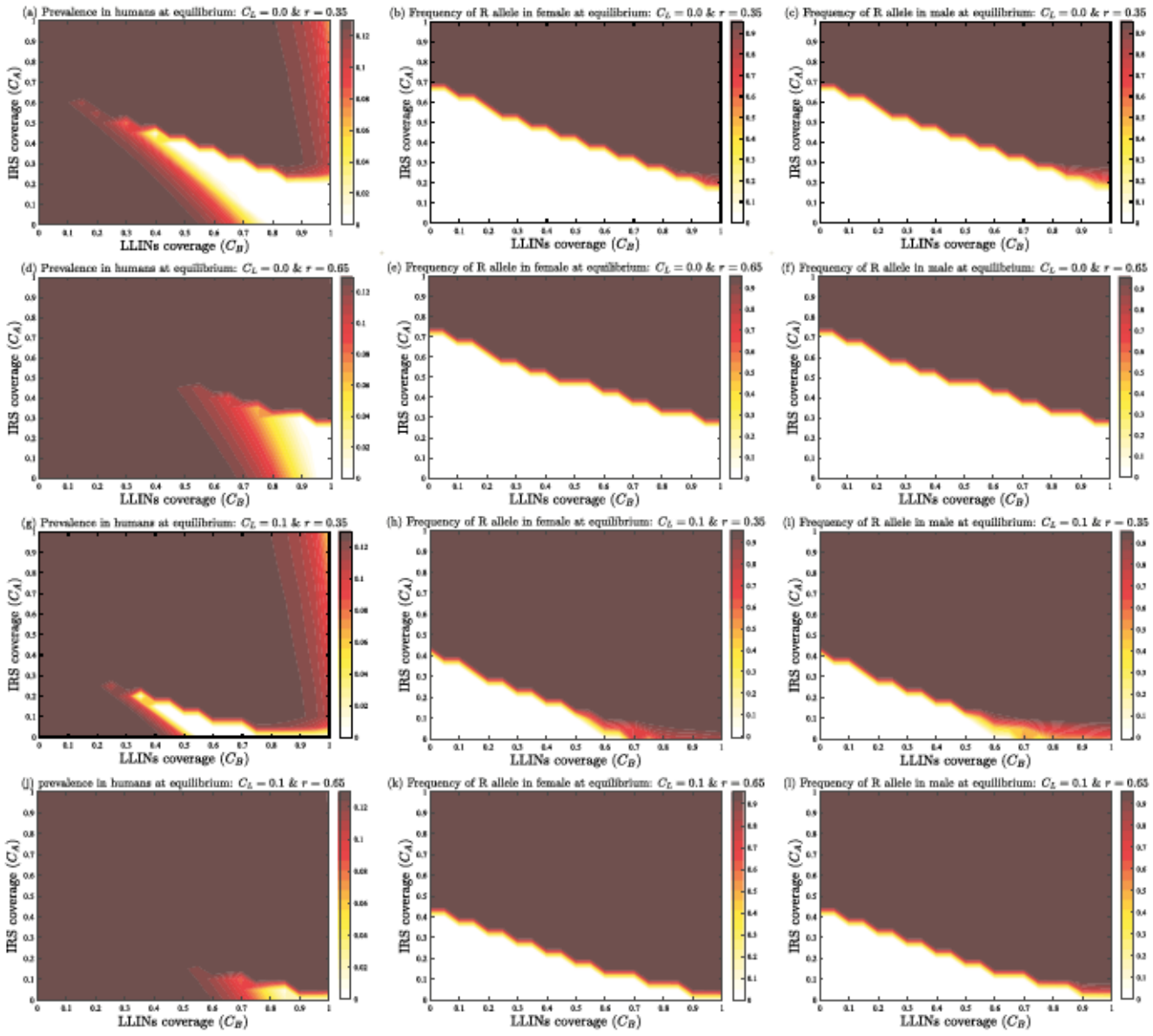

Fig. 4. Heat map of the model {(2.5)–(2.10)} for LLINs coverage (C_B) vs IRS coverage (C_A). Parameter values used are as given by the baseline values in Tables 2–4, with moderate initial resistant allele frequency given in (4.2). (i). (a)–(c) $C_L = 0$ and $r = 0.35$, (ii). (d)–(f) $C_L = 0$ and $r = 0.65$, (iii). (g)–(i) $C_L = 0.1$ and $r = 0.35$, (iv) (j)–(l) $C_L = 0.1$ and $r = 0.65$.

range $0.9 \leq C_B \leq 1$) can effectively control the disease and manage resistance, any addition of IRS coverage will lead to the failure of the combined LLINs-IRS program to control the disease or manage resistance (Fig. 4(j)–(k)).

The main reasoning behind the need to combine LLINs with IRS or larviciding (or with both IRS and larviciding) is to increase the likelihood that a mosquito interacts with an insecticide, and that such combination helps in reaching (and maintaining) high coverage levels of insecticide usage that are often difficult to achieve using singular implementation of any of the three insecticides-based mosquito control strategies [16]. This fact is vividly illustrated in our simulations. For example, with no larviciding, and with 35% of the new adult mosquitoes being females (i.e., $r = 0.35$), the use of LLINs alone can lead to effective control of malaria while also managing insecticide resistance if its coverage level is at least 77% (Fig. 4(a)–(c)). However, when larviciding coverage is increased to 10%, the (minimum) coverage level of LLINs needed to achieve both disease control and effective management of resistance is reduced to 53% (Fig. 4(g)–(i)). Furthermore, while keeping larviciding at 10%, if IRS at 18% coverage is used, the minimum level of LLINs coverage needed for achieving malaria control and effective resistance management is further reduced to 40% (Fig. 4(g)–(i)).

In general, altering the sex ratio in favor of male mosquitoes will greatly aid malaria elimination efforts even in the absence of insecticides. However, in our setting (in the absence of insecticide usage), we need much higher advantage in favor of male mosquitoes before such elimination can be achieved. For example, we need to reduce r to as low as $r = 0.03$ (i.e., 97% of new adult mosquitoes are males) to achieve elimination (i.e., bring and maintain the reproduction number less than unity). For the baseline parameter values used in our simulations (for the case with no insecticide usage), the associated basic reproduction number of the model takes the value $\mathcal{R}_{0_{SS}} = 111.83 > 1$. However, for this setting, if r is reduced to $r = 0.1$ (i.e., the proportion of new adult mosquitoes that are male is 90%), the basic reproduction number is reduced to $\bar{\mathcal{R}}_{0_{SS}} = 41.37 > 1$. Since the baseline setting is the high malaria transmission setting, $\mathcal{R}_{0_{SS}}$ is larger than unity even for values of r as low as $r = 0.05$. When r is further reduced,

e.g. to $r = 0.03$ (i.e., 97% of new adult mosquitoes are male), the system converges to the mosquito-free equilibrium (and the disease is eliminated). However, our simulations for moderate and low malaria transmission settings (without insecticide usage) suggest that malaria elimination is feasible for higher values of r (which may confirm the results in Galizi et al. [59]).

4.5. Assessing the population-level impact of initial size of resistant allele frequency

In this section, the model {(2.5)–(2.10)} is simulated to assess the population-level impact of the initial size of the resistant allele frequency on the effectiveness of a combined LLINs & IRS intervention. These simulations will be carried out for the case where larvicide intervention is not implemented (i.e., $C_L = 0$), to enable more emphasis on LLINs and IRS (the two primary mosquito control measures in endemic areas [6,7,16,18,22]).

For the case where the initial resistant allele frequency (as given in (4.1)) is low, simulations of the model show that LLINs alone, with high coverage (such as $0.9 \leq C_B \leq 1$) can lead to the effective control of malaria, while also effectively managing insecticide resistance (Fig. 5(a), (b), (c)). Furthermore, the effective management of resistance at this coverage level of LLINs coverage holds even if combined with IRS at moderate coverage level (e.g., $0 \leq C_A \leq 0.45$). The disease is effectively controlled if the LLINs-IRS coverage lies roughly in the region below the straight line joining the points $(C_B, C_A) = (0.4, 0, 8)$ and $(C_B, C_A) = (1, 0.5)$, and above the straight line joining the points $(0.4, 0.8)$ and $(0.9, 0)$ in the C_B–C_A plane (Fig. 5(a)). Outside this region, the disease is not controlled (although the disease prevalence is significantly reduced for LLINs-IRS coverage close to the borders of this region). Insecticide resistance is effectively managed when the LLINs-IRS coverage lies below the straight line joining the points $(C_B, C_A) = (0.14, 1)$ and $(1, 0.45)$ (Fig. 5(b) & (c)). Insecticide resistance is not effectively managed outside this region. For this setting with low initial frequency of resistant allele, our simulations show that malaria can be effectively controlled and insecticide resistance effectively managed if the LLINs-IRS coverage lies in the intersection of the aforementioned two regions. For this setting, lower LLINs coverage (up to $C_B = 0.4$) combined with IRS (with appropriate coverage level) can lead to the effective control of the disease, while also effectively managing insecticide resistance. For example, implementing an LLINs-IRS control with coverage level $(C_B, C_A) = (0.4, 0.8)$ can lead to such control and effectively manage insecticide resistance.

For moderate initial level of the resistant allele frequency (as given in (4.2)), our simulations show similar dynamics as obtained in Fig. 3(a), (b), (c).

For the case where the initial resistant allele frequency is high (as given in (4.3)), our simulations show that LLINs alone, at coverage of at least 90%, can lead to the effective control of the disease while also managing insecticide resistance effectively (Fig. 5(g), (h), (i)). Such management of insecticide resistance also holds if the LLINs (at this coverage level) is combined with IRS at coverage level within $0 \leq C_A \leq 0.21$. Further, the disease is effectively controlled if the coverage of the combined LLINs-IRS program lies roughly in the region below the straight line joining the points $(C_B, C_A) = (0.8, 0.23)$ and $(C_B, C_A) = (1, 0.18)$, and above the straight line joining the points $(C_B, C_A) = (0.8, 0.23)$ and $(C_B, C_A) = (0.9, 0)$ (Fig. 5(g)). Outside this region, the disease is not effectively controlled (*albeit* the disease prevalence is significantly reduced for LLINs-IRS coverage close to the borders of this region). Insecticide resistance is effectively managed when the LLINs-IRS coverage lies below the straight line joining the points $(C_B, C_A) = (0, 0.58)$ and $(C_B, C_A) = (1, 0.2)$ (Fig. 5(h) & (i)). Outside this region, insecticide resistance is not effectively managed. Here, too, the disease is effectively controlled, and insecticide resistance effectively managed, for LLINs-IRS coverage within the intersection of the aforementioned regions.

It can be concluded from the simulations in Fig. 5 that, for the various levels of the frequency of resistant allele considered, there is an effective control window in the LLINs-IRS coverage parameter space within which the combined LLINs-IRS strategy can lead to both the effective control of malaria and the effective management of insecticide resistance. The size of this effective control window significantly decreases with increasing values of the size of the initial resistant allele frequency. It is worth noting that the size of the effective control window is also negatively affected by increasing values of larviciding coverage (Fig. 3) and increasing values of the proportion of new adult mosquitoes that are females (Fig. 4). Furthermore, starting with LLINs and IRS coverage in the effective control window, any further increase in IRS coverage (outside its range of values within the effective control window) will lead to the failure of the insecticides-based control strategy to combat the disease as well as to effectively manage insecticide resistance (Figs. 3–5).

4.6. Assessing the impact of the level of dominance (h)

In this section, the potential impact of heterogeneity in the parameter (h) associated with the level of dominance of the resistant allele over the sensitive allele on the dynamics of the model {(2.5)–(2.10)} is assessed. In particular, the model is simulated subject to three different levels of this very important parameter. The simulations for the effect of the parameter h on the dynamics of the model are carried out for the special case of the model {(2.5)–(2.10)} in the absence of larvicides-based intervention (i.e., the larvicides coverage, C_L, is set to zero). This is done to enable more emphasis on LLINs and IRS (the two primary mosquito control measures in malaria-endemic areas with relatively low level of the initial resistant allele frequency (as given in (4.1))). For low value of the level of resistant allele dominance (i.e., $h = 0.25$) with low initial level of the resistant allele frequency (as given in (4.1)), the simulation results obtained are depicted in Fig. 5(a)–(c)) (and are discussed in Section 4.5).

When the level of the resistant allele dominance is increased from $h = 0.25$ to $h = 0.5$, the simulation results obtained show that the use of LLINs alone, with high coverage (such as C_B in the range $0.9 \leq C_B \leq 1$), can lead to the effective control of malaria, while also effectively managing insecticide resistance (Fig. 6(a), (b), (c)). In particular, malaria can be effectively controlled if the LLINs-IRS coverage pair lies roughly in the region below the straight line joining the points $(C_B, C_A) = (0.85, 0.15)$ and $(C_B, C_A) = (1, 0.2)$, and above the straight line joining the points $(0.85, 0.15)$ and $(0.9, 0)$ in the C_B–C_A plane (Fig. 6(a)). Outside this region, the disease cannot be effectively controlled (although the disease prevalence is significantly reduced for LLINs-IRS coverage close to the borders of this region). Furthermore, insecticide resistance is effectively managed when the LLINs-IRS coverage pair lies below the straight line joining the points $(C_B, C_A) = (0.0, 0.45)$ and $(1, 0.15)$ (Fig. 6(b) & (c)). It is also evident from this figure that insecticide resistance is not effectively managed outside this region. For this setting with low initial frequency of resistant allele, our simulations show that malaria can be effectively controlled, and insecticide resistance effectively managed, if the LLINs-IRS coverage pair lies in the intersection of the aforementioned two regions. It is clear, by comparing these results with the results obtained for the case with $h = 0.25$ (depicted in Fig. 5(a), (b), (c)), that the effective control window in the C_A–C_B plane is significantly reduced in (Fig. 6(a), (b), (c)) when the dominance of the resistance allele parameter h was increased to $h = 0.5$. In other words, increasing the dominance of the resistant allele, over the sensitive allele (from $h = 0.25$ to $h = 0.5$) resulted in a significant decrease in the size of the effective control window. Thus, increase h makes malaria elimination efforts more difficult.

When the dominance of the resistant allele parameter h is further increased to $h = 0.75$, the simulation results obtained show that LLINs alone can significantly reduce malaria burden (even though insecticide

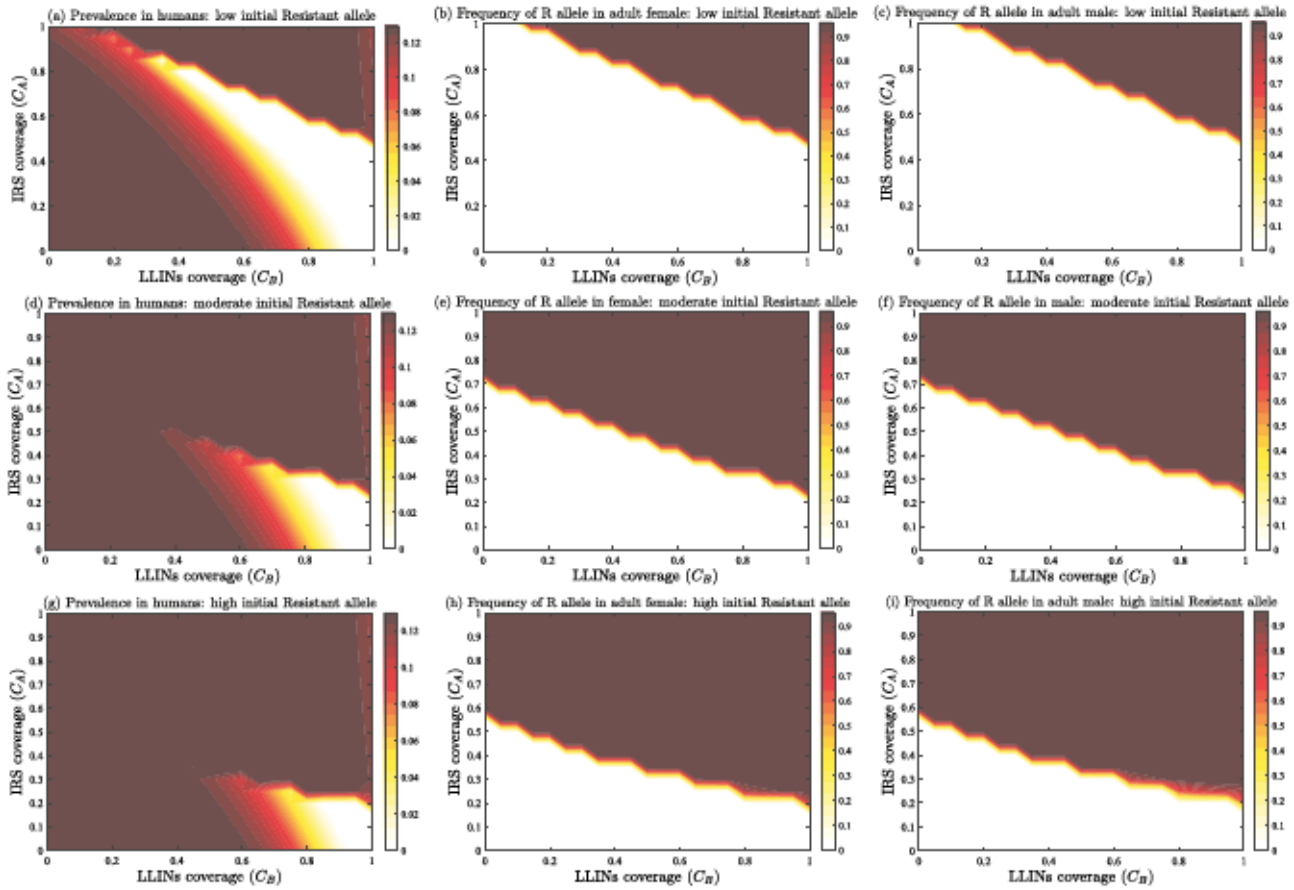

Fig. 5. Heat map of the model {(2.5)–(2.10)} for LLINs coverage (C_B) *vs.* IRS coverage (C_A). Parameter values used are as given by the baseline values in Tables 2–4, with no larvaciding $C_L = 0$. (i). (a)–(c) low initial resistant allele frequency given in (4.1), (ii). (d)–(f) moderate initial resistant allele frequency given in (4.2), and (iii). (g)–(i) high initial resistant allele frequency given in (4.3).

resistance is not effectively managed) when LLINs coverage (C_B) is close to 100% (Fig. 6(d)). Furthermore, while insecticide resistance is effectively managed when the LLINs-IRS coverage pair lies below the straight line joining the points $(C_B, C_A) = (0., 0.2)$ and $(0.4, 0.0)$ (Fig. 6(e) & (f)), such resistance is not effectively managed outside this region. For this setting (with low initial frequency of resistant allele and higher level of dominance value ($h = 0.75$)), there is no effective control window in the C_B–C_A plane where the disease is effectively controlled and insecticide resistance is effectively managed (Fig. 6(d), (e) & (f)). Furthermore, for this setting, when h is further increased to $h = 1$, the disease is not effectively controlled for all values of $0 \leq C_A \leq 1$ and $0 \leq C_B \leq 1$ in the C_A–C_B plane (Fig. 6(g)). In summary, simulations for this setting show that there is no effective control window in the C_B–C_A plane where the disease is effectively controlled and insecticide resistance effectively managed (Fig. 6(g), (h) & (i)).

In summary, for the setting with low initial frequency of resistant allele, our simulations show that, for low and moderate values of level of dominance h (for example for $h = 0.25$ & $h = 0.5$), there is an effective control window in the LLINs-IRS coverage parameter space within which the combined LLINs-IRS strategy can lead to both the effective control of malaria and the effective management of insecticide resistance (Figs. 5(a)–(c) & 6((a)–(c)). However, the size of this effective control window significantly decreases with increasing values of the level of dominance h. Furthermore, the simulations we carried out show that, for high values of level of dominance h (for example, for $h = 0.75$ or $h = 1$), there is no effective control window in the C_B–C_A plane where malaria is effectively controlled and insecticide resistance is effectively managed (as shown in Fig. 6(d)–(f) & ((g)–(i)).

Discussion and conclusions

Despite the major progress made in the battle against malaria from 2000 to 2015 [8], the disease continues to pose major public health and socio-economic burden in at least half the world's population [4,60–63]. For instance, data from the 2019 World Malaria Report shows that the disease accounted for an estimated 228 million infections and 405,000 deaths spread across 31 countries (mostly located in tropical and sub-tropical regions of the world) in 2018 (with sub-Saharan Africa bearing the brunt of the burden, suffering over 93% of the cases and 94% of the deaths) [63]. The progress recorded during the period 2000 to 2015 was owing to the wide-scale use of insecticides-based anti-malaria control measures, notably in the form of long-lasting insecticidal nets (LLINs) and indoor residual spraying (IRS), implemented in malaria-endemic areas [7,8,11,64,65]. Unfortunately, such wide-scale use of these interventions resulted in equally wide-spread mosquito resistance to nearly each of the five agents currently being used in LLINs and IRS [6,7,14,17,18,20,21,24]. There is now concerted global effort, such as The Global Technical Strategy for Malaria 2016–2030 and the $ZeroX40$ Initiative (an initiative of five chemical companies with the support of the Bill & Melinda Gates Foundation and the Innovative Vector Control Consortium [12,13]), aimed at eradicating malaria by 2030 or 2040. A critical question to ask is whether or not such eradication can be attained using the currently-available insecticides-based control measures. In other words, can the use of the currently-available insecticides lead to effective malaria control while also effectively managing insecticide resistance? Answering such a question will allow for the determination of whether or not such malaria eradication (by 2030 or 2040) is feasible using existing control resources. This study

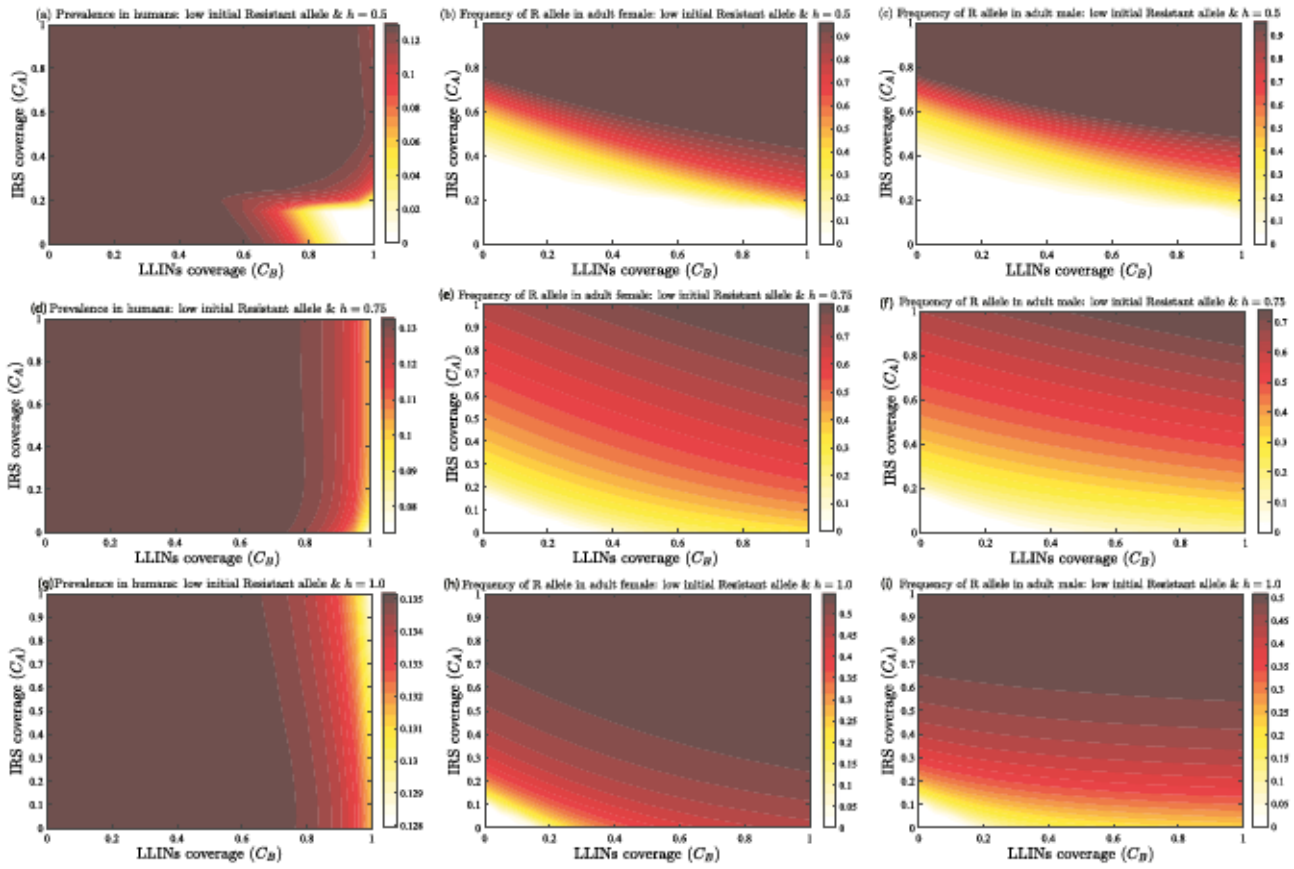

Fig. 6. Heat map of the model {(2.5)–(2.10)} for LLINs coverage (C_B) *vs.* IRS coverage (C_A). Parameter values used are as given by the baseline values in Tables 2–4, with no larvaciding $C_L = 0$ and low initial resistant allele frequency given in (4.1), for various values of level of dominance (h) (i). (a)–(c) $h = 0.5$, (ii). (d)–(f) $h = 0.75$, and (iii). (g)–(i) $h = 1.0$.

seeks to address this issue *via* the design, analysis and simulations of a novel mathematical model for malaria dynamics in a community.

The model developed in this study couples malaria epidemiology in humans (by including the dynamics of mosquito populations and humans) and the population genetics of the malaria vector (i.e., the population genetics of the *Anopheles* mosquito, *vis a vis* the evolution and spread of insecticide resistance). This modeling framework allows for the investigation of the disease dynamics and evolution of insecticide resistance simultaneously, in addition for the realistic assessment of the population-level impact of the three insecticides-based vector control measures (namely, the use of LLINs, IRS and larvicides). As noted by Barbosa et al. [15], the use of the aforementioned three insecticides-based vector control measures allows for the attainment of the high coverage levels of the vector control measures that are often difficult to attain if only one of the control measures is adopted. Some of the main novelties of the model developed in this study include explicitly incorporating the dynamics of aquatic (immature) mosquitoes (thereby allowing for the realistic assessment of larvicide-based control measures), the dynamics of male *Anopheles* mosquitoes (thereby allowing for the realistic accounting of the mating processes, as well as the assessment of the impact of altering the sex-ratio in the disease transmission and the evolution of insecticide resistance). Furthermore, since the development of resistance to an insecticide is associated with significant disadvantages that diminishes the mosquito's fitness (compared to its insecticide-sensitive counterparts in the population), the developed model also incorporates numerous pertinent fitness costs associated with insecticide resistance. These fitness costs include reduction in fecundity (growth rate) and increase in the natural mortality rate in heterozygous and homozygous resistant mosquitoes. Furthermore, the human population is stratified in terms of those who are protected (i.e., those who sleep under an LLIN) and those who are unprotected (i.e., those who do not sleep under a bednet). Furthermore, a new nonlinear mosquito biting rate function is introduced.

The developed model, which takes the form of a 29-dimensional deterministic system of nonlinear differential equations, was rigorously analyzed to gain insight into its dynamical features. In addition to establishing the well-posedness of the model (*via* the derivation of results for its non-negativity, boundedness and positive-invariance), it is shown that the non-trivial co-existence disease-free equilibrium of the model (when it exists) is locally-asymptotically stable whenever a certain epidemiological threshold quantity is less than unity. Further, for the special case of this equilibrium with no malaria-induced mortality in the human host population, this equilibrium is globally-asymptotically stable when the associated reproduction number is less than unity. The epidemiological consequence of the latter result is that malaria can be effectively controlled in the community if the associated reproduction can be reduced to (and maintained at) a value less than unity. In other case, for this special case of the model, this study shows that a wide-scale implementation of the currently-available insecticide-based interventions can lead to malaria elimination if they succeed in bringing (and maintaining) the associated reproduction number to a value less than unity.

The model was parametrized using data relevant to malaria transmission dynamics in the Jimma Zone of Southwestern Ethiopia [22, 54], and numerical simulations of the parametrized model were carried out to primarily assess the population-level impact of the three main pertinent quantities associated with effective malaria control and management of insecticide resistance, as described below:

(i) the impact of the interactions of the three insecticide-based anti-malaria control strategies (larvicide, LLINs and IRS) on disease control and insecticide resistance management;
(ii) the impact of the initial size of the vector sex ratio (i.e., the impact of the parameter governing the number of new adult mosquitoes that are females (r));
(iii) the impact of the initial size of the frequency of resistant allele in the community; and
(iv) the impact of the level of dominance (h).

Using moderate size of the initial resistant allele frequency in the community, our numerical simulations show that implementing LLINs alone can lead to the effective control (i.e., elimination) of malaria, while also effectively managing insecticide resistance, in the community if the LLINs coverage is very high. For example, for the ecological scenario with no IRS and larviciding, and with 50:50 adult mosquito sex ratio, LLINs at 90% coverage level can lead to the aforementioned effective control of the disease and resistance management. However, 90% LLINs coverage is certainly unrealistic in malaria-endemic areas. In fact, data from World Health Organization shows that LLINs coverage in malaria-endemic areas lie within the range of 40% to 80% [4]. Hence, LLINs (at realistic coverage level) are unable to singularly lead to the effective control of malaria (in addition to effectively managing insecticide resistance). However, as noted by Barbosa et al. [16], such effective control (and resistance management) can be achieved if LLINs (at realistic coverage range) are complemented with IRS and/or larviciding. Our simulations show, for instance, that LLINs at the reduced 80% coverage (i.e., the highly optimistic scenario based on the WHO estimate [4]) can lead to effective disease control and effective management of insecticide resistance if it is combined with IRS at 32% coverage (Fig. 3(a)–(c)). This result also holds if the proportion of new adult mosquitoes that are females is reduced from the 50% value to 35% (Fig. 4(g)–(i)).

For malaria-endemic communities with moderate frequency of resistance allele, our study shows, in the absence of larviciding, the existence of an *effective control window* in the LLINs-IRS coverage parameter space within which the combined use of LLINs and IRS can lead to the effective control of malaria, while also effectively managing insecticide resistance (Fig. 3). The size of this control window decreases with increasing values of the coverage level of larviciding (e.g., from 0% to as low as 10%). In other words, these simulations show that for malaria-endemic communities that are already implementing a malaria control strategy based on the combined use of LLINs and IRS, adding larviciding may threaten the gains made (by LLINs and IRS) for disease control and/or management of insecticide resistance. This result is intuitive, since an increase in the level of insecticides used in the community (in the form of LLINs, IRS and/or larvicides) certainly increases the likelihood of the emergence and spread of vector resistance to the insecticides (hence, threaten effective resistance management). Further, since resistant adult female mosquitoes are no longer affected by the insecticides-based control measures, these mosquitoes (if infected with malaria) will continue to transmit the disease to humans unabated (by LLINs or IRS), thereby threatening efforts for effective malaria control. It is further shown that, for LLINs and IRS coverage levels within the effective control window, any further increase in IRS coverage may lead to the failure of the insecticides-based intervention in the community. This result is consistent with that reported in the modeling study by Barbosa et al. [16], which showed that insecticide resistance spreads faster when the insecticides target the larval stages of the immature mosquito lifecycle (i.e., resistance spreads faster when larvicides are used). Their result is intuitive because larvicides do not kill adult mosquitoes that are potentially infectious (which implies that larvicides have a smaller impact on reducing disease transmission) and larviciding applies selection pressure for resistance on both sexes (thereby leading to faster spread of insecticide resistance) [16]. Similarly, since IRS affects both adult female and male mosquitoes, it applies selection pressure on both sexes (hence, IRS also leads to faster spread of insecticide resistance). Furthermore, unlike LLINs and IRS, larviciding will not reduce the longevity of adult female mosquitoes [16].

Simulations were carried out to assess the community-wide impact of the adult mosquito sex ratio (as modeled by the parameter r, for the number of new adult mosquitoes that are females, in our study). For the case where larvicides were not used, and for moderate initial size of the resistant allele in the community, the simulation results obtained showed that the combined use of LLINs and IRS can lead to the effective control of the disease, while also effectively managing resistance, if the value of r is small enough (e.g., ≤ 0.35). Furthermore, the size of the associated effective control window (in the parameter space for the combined LLINs-IRS coverage) decreased with increasing values of r (Fig. 4). This result was expected, since the larger the proportion of new adult mosquitoes that are females, the more difficult it would be to effectively control the disease and manage insecticide resistance. The simulations also showed that a further increase in IRS coverage may be counterproductive. For instance, in the absence of larviciding and with $r = 0.35$ and LLINs coverage at 77%, Fig. 4 showed that both the disease and insecticide resistance can be effectively controlled if the IRS coverage was low enough (less than 27%). However, if the IRS coverage was increased above 27%, such effective control of the disease and resistance were no longer feasible. Similar result was reported by Barbosa et al. [16], which emphasized that if IRS coverage is low (noting that for $r = 0.35$, the proportion of new adult mosquitoes that are males is 65%), then the larger insecticide-sensitive adult male mosquito population will be largely maintained in the community (since the adult male mosquito population is only affected by IRS and not by LLINs or larviciding). In this case, owing to the abundance of sensitive mosquitoes in the community/environment, the use of insecticides will (in general) be helpful in effectively controlling the mosquito population (hence, controlling the disease spread). However, increasing IRS coverage further (above its range within the associated effective control window) will lead to high selection pressure for insecticide resistance (thereby leading to the failure of the control intervention) [16,22].

Simulations for assessing the community-wide impact of the initial size of the resistant allele frequency show that there is a region in the parameter space for the LLINs-IRS coverage within which the implementation of the combined LLINs-IRS can lead to both effective malaria control and effective management of insecticide resistance. The size of this region significantly decreases with increasing values of the size of the initial resistant allele frequency (Fig. 5). In other words, this study shows that for malaria-endemic communities with high frequency of resistant allele, the implementation of a control strategy based on using LLINs and IRS (with high coverages) can make things worse, *vis a vis* malaria control and management of insecticide resistance. This result can intuitively be explained based on the reasoning that for a malaria-endemic community with high initial frequency of resistant allele, the extensive and wide-scale use of insecticides-based interventions (i.e., high coverage of IRS, LLINs and larviciding and/or their combinations) could lead to high selection pressure (for insecticide resistance) and the overall failure of the insecticides-based control measures implemented in the community [16,22].

Simulations are carried out to assess the community-wide impact of the level of dominance parameter h. Using moderate size of the initial resistant allele frequency in the community. Our numerical simulations show that for low and moderate values of level of dominance h (for example for $h = 0.25$ & $h = 0.5$), there is an effective control window in the LLINs-IRS coverage parameter space within which the combined LLINs-IRS strategy can lead to both the effective control of malaria and the effective management of insecticide resistance (Figs. 5(a)–(c) & 6((a)–(c)). However, the size of this effective control window significantly decreases with increasing values of the level of dominance h. Furthermore, the simulations show that for high values of level of dominance h (for example for $h = 0.75$ & $h = 1$), there is no effective

control window in the C_A–C_B plane where the disease is effectively controlled and insecticide is effectively managed (in Fig. 6(d)–(f) & ((g)–(i)).

The simulations carried out in this study (depicted in Figs. 3–6) clearly emphasize the importance of numerous parameters of the model on the transmission dynamics of the disease and the management of resistance. The simulations show that parameters such as those associated with the coverage for larvicide (C_L), IRS (C_A), LLINs (C_B), the proportion of new adult mosquitoes that are females (r) and the initial size of the resistant allele frequency in the community ($p_f(0)$ and $p_m(0)$) have non-linear (and complex) effect on the disease dynamics and the evolution of insecticide resistance. In particular, this study identifies three main mechanisms that greatly threaten the effectiveness of an anti-malaria intervention based on the combined use of LLINs and IRS (the two cornerstone vector control interventions for the current malaria eradication drive), by reducing (or eliminating) the size of the associated effective control window in the LLINs-IRS coverage parameter space. These are increases in (i) larviciding coverage (C_L), (ii) proportion of new adult female mosquitoes that are females (r) and (iii) the initial size of the frequency of resistant allele in the community ($p_f(0)$ and $p_m(0)$). Thus, it is crucial that these parameters are realistically-estimated (using clinical and field data) in order to further investigate their effect on the transmission dynamics of malaria and on the emergence and spread of insecticide resistance. Similar clinical and field data are also crucially needed for realistically-estimating some of the parameters related to the fitness cost of insecticide resistance. In particular, as noted by Mohammed-Awel and Gumel [22], the fitness costs associated with insecticide resistance and the allele dominance (h) parameters have important roles in the disease dynamics and evolution of insecticide resistance. Thus, to further gain realistic insight into the connection between malaria epidemiology and insecticide resistance, further modeling work needs to be done and backed by data to realistically estimate some of the pertinent parameters (such as the aforementioned). It is worth mentioning that the model we developed in this study does not account for the residual exposure of *Anopheles* mosquitoes to the pesticides/insecticides used in agriculture (e.g., the use of pesticides or insecticides against insects that affect crops). This was a simplifying assumption made to enable the already complex model we developed to be mathematically-tractable (and we plan to relax this assumption in a later study). In summary, this study shows that malaria can be effectively controlled, while insecticide resistance is also effectively managed, using existing LLINs-IRS-based interventions if their coverage levels are chosen within the identified effective control window in the LLINs-IRS coverage parameter space. In other words, the concerted global effort to eradicate malaria by 2030 or 2040 is feasible, using the combined LLINs-IRS strategy, if the coverage levels for LLINs and IRS are carefully chosen (to lie within the control window). Our study further emphasize the importance of prioritizing investments on LLINs, rather than on IRS (since the former is demonstratively the main mechanism for malaria control).

Declaration of competing interest

The authors declare that they have no known competing financial interests or personal relationships that could have appeared to influence the work reported in this paper.

Acknowledgments

Two of the authors (ABG and JMA) are grateful to National Institute for Mathematical and Biological Synthesis (NIMBioS), USA for funding the Working Group on Climate Change and Vector-borne Diseases (VBDs). NIMBioS is an Institute sponsored by the National Science Foundation, USA, the U.S. Department of Homeland Security, and the U.S. Department of Agriculture through NSF Award #EF-0832858, with additional support from The University of Tennessee, Knoxville, USA. ABG also acknowledges the support, in part, of the Simons Foundation, USA (Award #585022). The authors are very grateful to the two anonymous reviewers for their very constructive comments, which have significantly enhanced the manuscript.

Appendix. Proof of Theorem 3.4

Proof. Consider the special case of the model {(2.5)–(2.10)} without disease-induced mortality in the host population (i.e., $\delta_H = 0$). Further, let $\mathcal{R}_{SS} > 1$ and $\mathcal{R}_{RR} > 1$ (so that $\mathcal{T}_4$, exists) and $\mathcal{R}_{0C} \leq 1$. Setting $\delta_H = 0$ in the model {(2.5)–(2.10)} gives $N_H(t) \to \frac{\Pi_H}{\mu_H}$ as $t \to \infty$, and $\bar{K}_{20} = \gamma_H + \mu_H$. Hence, from now on, $N_H(t)$ is replaced by its limiting value, $\frac{\Pi_H}{\mu_H}$. The equations for the infected components of the special case of the model {(2.5)–(2.10)} can be written in matrix–vector form:

$$\begin{pmatrix} \dot{E}^f_{SS}(t) \\ \dot{I}^f_{SS}(t) \\ \dot{E}^f_{RS}(t) \\ \dot{I}^f_{RS}(t) \\ \dot{E}^f_{RR}(t) \\ \dot{I}^f_{RR}(t) \\ \dot{E}_{Hp}(t) \\ \dot{I}_{Hp}(t) \\ \dot{E}_{Hu}(t) \\ \dot{I}_{Hu}(t) \end{pmatrix} = \left[(F - V) - \left(1 - \frac{S_{Hp}}{N_H}\right) J_1 - \left(1 - \frac{S_{Hu}}{N_H}\right) J_2 - J_3\right] \begin{pmatrix} E^f_{SS}(t) \\ I^f_{SS}(t) \\ E^f_{RS}(t) \\ I^f_{RS}(t) \\ E^f_{RR}(t) \\ I^f_{RR}(t) \\ E_{Hp}(t) \\ I_{Hp}(t) \\ E_{Hu}(t) \\ I_{Hu}(t) \end{pmatrix}, \tag{A.1}$$

where the matrices F and V are as defined in Section 3.1, and the matrices J_1, J_2 and J_3 are given, respectively, by:

$$J_1 = \begin{bmatrix} 0 & 0 & 0 & 0 & 0 & 0 & 0 & 0 & 0 & 0 \\ 0 & 0 & 0 & 0 & 0 & 0 & 0 & 0 & 0 & 0 \\ 0 & 0 & 0 & 0 & 0 & 0 & 0 & 0 & 0 & 0 \\ 0 & 0 & 0 & 0 & 0 & 0 & 0 & 0 & 0 & 0 \\ 0 & 0 & 0 & 0 & 0 & 0 & 0 & 0 & 0 & 0 \\ 0 & 0 & 0 & 0 & 0 & 0 & 0 & 0 & 0 & 0 \\ 0 & \beta_H b_{SS} C_B & 0 & \beta_H b_{RS} C_B & 0 & \beta_H b_{RR} C_B & 0 & 0 & 0 & 0 \\ 0 & 0 & 0 & 0 & 0 & 0 & 0 & 0 & 0 & 0 \\ 0 & 0 & 0 & 0 & 0 & 0 & 0 & 0 & 0 & 0 \\ 0 & 0 & 0 & 0 & 0 & 0 & 0 & 0 & 0 & 0 \end{bmatrix},$$

$$J_2 = \begin{bmatrix} 0 & 0 & 0 & 0 & 0 & 0 & 0 & 0 & 0 & 0 \\ 0 & 0 & 0 & 0 & 0 & 0 & 0 & 0 & 0 & 0 \\ 0 & 0 & 0 & 0 & 0 & 0 & 0 & 0 & 0 & 0 \\ 0 & 0 & 0 & 0 & 0 & 0 & 0 & 0 & 0 & 0 \\ 0 & 0 & 0 & 0 & 0 & 0 & 0 & 0 & 0 & 0 \\ 0 & 0 & 0 & 0 & 0 & 0 & 0 & 0 & 0 & 0 \\ 0 & 0 & 0 & 0 & 0 & 0 & 0 & 0 & 0 & 0 \\ 0 & 0 & 0 & 0 & 0 & 0 & 0 & 0 & 0 & 0 \\ 0 & \beta_H b_{\max}(1 - C_B) & 0 & \beta_H b_{\max}(1 - C_B) & 0 & \beta_H b_{\max}(1 - C_B) & 0 & 0 & 0 & 0 \\ 0 & 0 & 0 & 0 & 0 & 0 & 0 & 0 & 0 & 0 \end{bmatrix},$$

$$J_3 = \begin{bmatrix} 0 & 0 & 0 & 0 & 0 & 0 & 0 & \frac{\beta_V \nu_H b_{SS}(S_{SS}^{f***} - S_{SS}^{f})}{\Pi_H} & 0 & \frac{\beta_V \nu_H b_{max}(S_{SS}^{f***} - S_{SS}^{f})}{\Pi_H} \\ 0 & 0 & 0 & 0 & 0 & 0 & 0 & 0 & 0 & 0 \\ 0 & 0 & 0 & 0 & 0 & 0 & 0 & \frac{\beta_V \nu_H b_{RS}(S_{RS}^{f***} - S_{RS}^{f})}{\Pi_H} & 0 & \frac{\beta_V \nu_H b_{max}(S_{RS}^{f***} - S_{RS}^{f})}{\Pi_H} \\ 0 & 0 & 0 & 0 & 0 & 0 & 0 & 0 & 0 & 0 \\ 0 & 0 & 0 & 0 & 0 & 0 & 0 & \frac{\beta_V \nu_H b_{RR}(S_{RR}^{f***} - S_{RR}^{f})}{\Pi_H} & 0 & \frac{\beta_V \nu_H b_{max}(S_{RR}^{f***} - S_{RR}^{f})}{\Pi_H} \\ 0 & 0 & 0 & 0 & 0 & 0 & 0 & 0 & 0 & 0 \\ 0 & 0 & 0 & 0 & 0 & 0 & 0 & 0 & 0 & 0 \\ 0 & 0 & 0 & 0 & 0 & 0 & 0 & 0 & 0 & 0 \\ 0 & 0 & 0 & 0 & 0 & 0 & 0 & 0 & 0 & 0 \\ 0 & 0 & 0 & 0 & 0 & 0 & 0 & 0 & 0 & 0 \end{bmatrix}.$$

Since $S_{H_p}(t) \leq N_H$, $S_{H_u}(t) \leq N_H$, $S_{SS}^f \leq S_{SS}^{f***}$, $S_{RS}^f \leq S_{RS}^{f***}$, $S_{RR}^f \leq S_{RR}^{f***}$, $N_H(t) = \frac{\Pi_H}{\mu_H}$ in $\Omega \setminus (\mathcal{T}_1 \cup \mathcal{T}_2 \cup \mathcal{T}_3)$ for all $t > 0$, and the fact that the matrix J_3 is non-negative. It follows that:

$$\begin{pmatrix} \dot{E}_{SS}^f(t) \\ \dot{I}_{SS}^f(t) \\ \dot{E}_{RS}^f(t) \\ \dot{I}_{RS}^f(t) \\ \dot{E}_{RR}^f(t) \\ \dot{I}_{RR}^f(t) \\ \dot{E}_{H_p}(t) \\ \dot{I}_{H_p}(t) \\ \dot{E}_{H_u}(t) \\ \dot{I}_{H_u}(t) \end{pmatrix} \leq (F - V) \begin{pmatrix} E_{SS}^f(t) \\ I_{SS}^f(t) \\ E_{RS}^f(t) \\ I_{RS}^f(t) \\ E_{RR}^f(t) \\ I_{RR}^f(t) \\ E_{H_p}(t) \\ I_{H_p}(t) \\ E_{H_u}(t) \\ I_{H_u}(t) \end{pmatrix}. \tag{A.2}$$

Furthermore, since all the eigenvalues of $F - V$ have negative real part for $\mathcal{R}_{0C} < 1$ (from the local stability result in Theorem 3.2), it follows that the linearized system of differential inequality (A.2) is stable if $\mathcal{R}_{0C} < 1$. That is, substituting $E_{SS}^f(t) = I_{SS}^f(t) = E_{RS}^f(t) = I_{RS}^f(t) = E_{RR}^f(t) = I_{RR}^f(t) = E_{H_p}(t) = I_{H_p}(t) = E_{H_u}(t) = I_{H_u}(t) = 0$ into the equations of the special case of the model {(2.5)–(2.10)} gives:

$$\begin{aligned} &\left(E_{SS}^f(t), I_{SS}^f(t), E_{RS}^f(t), I_{RS}^f(t), E_{RR}^f(t), I_{RR}^f(t),\right. \\ &\left. E_{H_p}(t), I_{H_p}(t), R_{H_p}(t), E_{H_u}(t), I_{H_u}(t), R_{H_u}(t)\right) \\ &\to (0,0,0,0,0,0,0,0,0,0,0,0) \text{ as } t \to \infty. \end{aligned}$$

Thus,

$$\begin{aligned} B(t) \longrightarrow \Bigg(&E_{SS}^{f***}, E_{RS}^{f***}, E_{RR}^{f***}, L_{SS}^{***}, L_{RS}^{***}, L_{RR}^{***}, P_{SS}^{***}, P_{RS}^{***}, P_{RR}^{***}, M_{SS}^{m***}, \\ &M_{RS}^{m***}, M_{RR}^{m***}, S_{SS}^{f***}, 0, 0, S_{RS}^{f***}, 0, 0, S_{RR}^{f***}, 0, 0, \frac{C_B \Pi_H}{\mu_H}, \\ &0, 0, 0, \frac{(1 - C_B)\Pi_H}{\mu_H}, 0, 0, 0\Bigg), \end{aligned}$$

as $t \to \infty$ for $\mathcal{R}_{0C} \leq 1$. Hence, the NTCDFE, $\mathcal{T}_4$, is globally-asymptotically stable in $\Omega \setminus (\mathcal{T}_1 \cup \mathcal{T}_2 \cup \mathcal{T}_3)$ if $\mathcal{R}_{0C} \leq 1$ for the special case of the model {(2.5)–(2.10)} with $\delta_H = 0$. □

It is worth mentioning that the global asymptotic stability analysis of the other non-trivial disease-free equilibria, $\mathcal{T}_2$ and $\mathcal{T}_3$ (i.e., the results in Theorem 3.5), can also be proved using a similar approach (hence, not repeated).

References

[1] P.W. Gething, A.P. Patil, D.L. Smith, C.A. Guerra, I.R. Elyazar, G.L. Johnston, A.J. Tatem, S.I. Hay, A new world malaria map: *Plasmodium falciparum* endemicity in 2010, Malar. J. 10 (2011) 378.

[2] G.L. Johnston, D.L. Smith, D.A. Fidock, Malaria's missing number: calculating the human component of R by a within-host mechanistic model of *Plasmodium falciparum* infection and transmission, PLoS Comput. Biol. 9 (4) (2013) e1003025, http://dx.doi.org/10.1371/journal.pcbi.1003025.

[3] D.E. Loy, W. Liu, Y. Li, G.H. Learn, L.J. Plenderleith, S.A. Sundararaman, P.M. Sharp, Hahn B.H., Out of Africa: origins and evolution of the human malaria parasites *Plasmodium falciparum* and *Plasmodium vivax*, J. Parasitol. 47 (2–3) (2017) 87–97.

[4] World Health Organization, World Malaria Report 2019, 2019, https://www.who.int/news-room/feature-stories/detail/world-malaria-report-2019. Accessed: 2019.

[5] L.M. Beck-Johnson, W.A. Nelson, K.P. Paaijmans, A.F. Read, M.B. Thomas, O.N. Bjørnstad, The importance of temperature fluctuations in understanding mosquito population dynamics and malaria risk, R. Soc. Open Sci. 4 (2017) 160969, http://dx.doi.org/10.1098/rsos.160969.

[6] S.E. Eikenberry, A.B. Gumel, Mathematical modeling of climate change and malaria transmission dynamics: a historical review, J. Math. Biol. (2018) http://dx.doi.org/10.1007/s00285-018-1229-7.

[7] S. Huijben, K.P. Paaijmans, Putting evolution in elimination: Winning our ongoing battle with evolving malaria mosquitoes and parasites, Evol. Appl. (2017) 1–16, Special Issue.

[8] J.M. Riveron, M. Tchoualaui, L. Mugenzi, B.D. Menze, M.-C. Chiang, C.S. Wondji, Insecticide resistance in malaria vectors: An update at a global scale, in: Towards Malaria Elimination - a Leap Forward (Sylvie Manguin and Vas Dev Editors), 2018.

[9] World Health Organization, Global technical strategy for Malaria 2016–2030, 2015, Retrieved from http://www.who.int/malaria/publications/atoz/9789241564991/en/.

[10] B. Kabula, W. Kisinza, P. Tungu, C. Ndege, B. Batengana, D. Kollo, R. Malima, J. Kafuko, M. Mohamed, S. Magesa, Cooccurrence and distribution of East (L1014S) and West (L1014F) African knockdown resistance in anopheles gambiae sensu lato population of Tanzania, Trop. Med. Int. Health 19 (3) (2014) 331–341.

[11] S. Bhatt, D.J. Weiss, E. Cameron, D. Bisanzio, B. Mappin, U. Dalrymple, K. Battle, C.L. Moyes, A. Henry, P.A. Eckhoff, E.A. Wenger, O. Briët, M.A. Penny, T.A. Smith, A. Bennett, J. Yukich, T.P. Eisele, J.T. Griffin, C.A. Fergus, M. Lynch, F. Lindgren, J.M. Cohen, C.L.J. Murray, D.L. Smith, S.I. Hay, R.E. Cibulskis, P.W. Gething, The effect of malaria control on *Plasmodium falciparum* in africa between 2000 and 2015, Nature 526 (2015) 207–211.

[12] Gates Foundation, Malaria strategy overview, 2019, Accessed, 2019. https://www.gatesfoundation.org/What-We-Do/Global-Health/Malaria.

[13] D.W. Willis, N. Hamon, Eliminating malaria by 2040 among agricultural households in africa; potential impact on health, labor productivity, education and gender equality, Gates Open Res. 2 (33) (2018) http://dx.doi.org/10.12688/gatesopenres.12843.2.

[14] H. Alout, B. Roche, R.K. Dabiré, A. Cohuet, Consequences of insecticide resistance on malaria transmission, PLoS Pathog. 13 (9) (2017) e1006499.

[15] S. Barbosa, I.M. Hastings, The importance of modeling the spread of insecticide resistance in a heterogeneous environment: the example of adding synergists to bednets, Malar. J. 11 (2012) 258.

[16] S. Barbosa, K. Kay, N. Chitnis, I. Hastings, Modelling the impact of insecticide-based control interventions on the evolution of insecticide resistance and disease transmission, Parasites Vectors 11 (2018) 482, http://dx.doi.org/10.1186/s13071-018-3025-z.

[17] A.M. Dondorp, F. Nosten, P. Yi, D. Das, A.P. Phyo, J. Tarning, et al., Artemisinin resistance in *Plasmodium falciparum* malaria, New Engl. J. Med. 361 (5) (2009) 455–467.

[18] S.E. Eikenberry, A. Gumel, A mathematics of malaria and climate change, in: Hans G. Kaper, Fred S. Roberts (Eds.), Book Chapter in Mathematics of Planet Earth: Protecting Our Planet, Learning from the Past, Safeguarding the Future, Springer International Publishing AG, 2018, pp. 67–89.

[19] J. Hemingway, H. Ranson, A. Magill, J. Kolaczinski, C. Fornadel, J. Gimnig, M. Coetzee, F. Simard, D.K. Roch, C.K. Hinzoumbe, J. Pickett, Averting a malaria disaster: will insecticide resistance derail malaria control? Lancet 387 (10029) (2016) 1785–1788.

[20] M. Imwong, K. Suwannasin, C. Kunasol, K. Sutawong, M. Mayxay, H. Rekol, et al., The spread of artemisinin-resistant *Plasmodium falciparum* in the greater mekong subregion: a molecular epidemiology observational study, Lancet Infec. Dis. (2017) http://dx.doi.org/10.1016/S1473-3099(17)30048-8.

[21] World Health Organization, Global Database on Insecticide Resistance in Malaria Vectors, 2020, https://www.who.int/malaria/areas/vector_control/insecticide_resistance_database/en/.

[22] J. Mohammed-Awel, A.B. Gumel, Mathematics of an epidemiology-genetics model for assessing the role of insecticides resistance on malaria transmission dynamics, Math. Biosci. 312 (2019) 33–49, June 2019, https://www.sciencedirect.com/science/article/abs/pii/S0025556417306636?via%3Dihub.

[23] H. Alout, P. Labbe, F. Chandre, A. Cohuet, Malaria vector control still matters despite insecticide resistance, Trends Parasitol. 33 (8) (2017).

[24] I. Enahoro, E. Eikenberry, A.B. Gumel, S. Huijben, K. Paaijmans, Long-lasting insecticidal nets and the quest for malaria eradication: A mathematical modeling approach, J. Math. Biol. (2020) in press.

[25] I. Kleinschmidt, J. Bradley, T. Knox, A.P. Mnzava, H. Kafy, et al., 2018. Implications of insecticide resistance for malaria vector control with long-lasting insecticidal nets: a WHO-coordinated, prospective, international, observational cohort study. 18(6)640-649.
[26] E. Ochomo, M. Chahilu, J. Cook, T. Kinyari, N. Bayoh, et al., Insecticide-treated nets and protection against insecticide- resistant malaria vectors in western Kenya, Emerg. Infect. Diseases 23 (5) (2017).
[27] R. Maharaj, D.J. Mthembu, B.L. Sharp, Impact of DDT re-introduction on malaria transmission in KwaZulu-Natal, S. Afr. Med. J. 95 (11) (2005) 871–874.
[28] N. Platt, R.M. Kwiatkowska, H. Irving, A. Diabaté, R. Dabire, C.S. Wondji, Target-site resistance mutations (kdr and RDL), but not metabolic resistance, negatively impact male mating competiveness in the malaria vector Anopheles gambiae, Heredity 115 (3) (2015) 243–252.
[29] M. Kuniyoshi, F. Santos, Mathematical modelling of vector-borne diseases and insecticide resistance evolution, J. Venom. Anim. Toxins Incl. Trop. Dis. 23 (2017) 34.
[30] P.L.G. Birget, J.C. Koella, A genetic model of the effects of insecticide-treated bed nets on the evolution of insecticide-resistance, Evol. Med. Public Health 20 (2015) 5–215.
[31] Z.S. Brown, K.L. Dickinson, R.A.R.A. Kramer, Insecticide resistance and malaria vector control: The importance of fitness cost mechanisms in determining economically optimal control trajectories, J. Econ. Entomol. 106 (1) (2013) 366–374.
[32] H. Alout, R.K. Dabire, L.S. Djogbénou, L. Abste, V. Corbel, F. Chandre, A. Cohuet, Interactive cost of *Plasmodium infection* and insecticide resistance in the malaria vector *Anopheles gambiae*, Sci. Rep. 6 (2016) 29755, 1-11.
[33] A. Asale, Y. Getachew, W. Hailesilassie, N. Speybroeck, L. Duchateau, D. Yewhalaw, Evaluation of the efficacy of DDT indoor residual spraying and long-lasting insecticidal nets against insecticide resistant populations of *Anopheles arabiensis Patton* (*Diptera: Culicidae*) from Ethiopia using experimental huts, Parasites Vectors 7 (2017) 131.
[34] O.J.T. Briet, M.A. Penny, D. Hardy, T.S. Awolola, W.B. Bortel, V. Corbel, R.K. Dabire, J. Etang, B.G. Koudou, P.K. Tungu, N. Chitnis, Effects of pyrethroid resistance on the cost effectiveness of a mass distribution of longlasting insecticidal nets: a modelling study, Malar. J. 12 (2013) 77, http://www.malariajournal.com/content/12/1/77.
[35] B. Levick, A. South, I.A. Hastings, A two-locus model of the evolution of insecticide resistance to inform and optimise public health insecticide deployment strategies, PLoS Comput. Biol. 13 (1) (2017) e1005327, http://dx.doi.org/10.1371/journal.pcbi.1005327.
[36] J. Mohammed-Awel, F. Agusto, R.E. Mickens, A.B. Gumel, Mathematical assessment of the role of vector insecticide resistance and feeding/resting behavior on malaria transmission dynamics: Optimal control analysis, Infec. Dis. Modell. 3 (2018) 301–321, https://www.ncbi.nlm.nih.gov/pmc/articles/PMC6326232/pdf/main.pdf.
[37] A. Hastings, Population Biology: Concepts and Models, first ed., Springer, New York, 1997.
[38] K. Okuneye, E. Eikenberry, A. Gumel, Weather-driven malaria transmission model with gonotrophic and sporogonic cycles, J. Biol. Dyn. (2019) in press.
[39] A.M. Lutambi, M.A. Penny, T. Smith, N. Chitnis, Mathematical modelling of mosquito dispersal in a heterogeneous environment, Math. Biosci. 241 (2013) 198–216.
[40] H. Wan, H. Zhu, A new model with delay for mosquito population dynamics, Math. Biosci. Eng. 11 (6) (2014) 1395–1410.
[41] C.N. Ngonghala, S.Y. Del Valle, R. Zhao, J. Mohammed-Awel, Quantifying the impact of decay in bednets efficacy on malaria transmission, J. Theoret. Biol. 364 (2014) 247–261.
[42] L.M. Childs, F.Y. Cai, E.G. Kakani, S.N. Mitche, D. Paton, P. Gabrieli, C.O. Buckee, F. Catteruccia, Disrupting mosquito reproduction and parasite development for Malaria control, PLoS Pathog. 12 (12) (2016) e1006060, http://dx.doi.org/10.1371/journal.ppat.1006060.
[43] S. Bala, B. Gimba, Global sensitivity analysis to study the impacts of bednets, drug treatment, and their efficacies on a two-strain malaria model, Math. Comput. Appl. 24 (32) (2019) 1–28.
[44] K.W. Blayneh, J. Mohammed-Awel, Insecticide-resistant mosquitoes and malaria control, Math. Biosci. 252 (2014) 14–26.
[45] S.A. Gourley, R. Liu, J. Wu, Slowing the evolution of insecticide resistance in mosquitoes: a mathematical model, Proc. R. Soc. Lond. Ser. A Math. Phys. Eng. Sci. 467 (2011) 2127–2148.
[46] A. South, I.A. Hastings, Insecticide resistance evolution with mixtures and sequences: a model-based explanation, Malar. J. 17 (2018) 80, http://dx.doi.org/10.1186/s12936-018-2203-y.
[47] J. Wairimu, M. Ronoh, Modeling insecticide resistance in endemic regions of Kenya, Appl. Math. 7 (2016) 542–555.
[48] F.B. Agusto, S.Y.D. Valle, K.W. Blayneh, C.N. Ngonghala, M.J. Goncalves, N. Li, R. Zhao, H. Gong, The impact of bednet use on malaria prevalence, J. Theoret. Biol. 320 (2013) 58–65.
[49] J. Mohammed-Awel, R. Zhao, E. Numfor, S. Lenhart, Management strategies in a Malaria model combining human and transmission-blocking vaccines, Discrete Contin. Dyn. Syst. - Ser. B (DCDS-B) 22 (3) (2017) 977–1000.
[50] J. Mohammed-Awel, E. Numfor, Optimal insecticide treated bednet coverage and Malaria treatment in a Malaria-HIV Co-infection model, J. Biol. Dyn. 11 (2017) 160–191.
[51] C.N. Ngonghala, J. Mohammed, R. Zhao, O. Prosper, Interplay between insecticide-treated bednets and mosquito demography: implications for malaria control, J. Theoret. Biol. 397 (2016) 179–192.
[52] O. Diekmann, J.A.P. Heesterbeek, J.A.J. Metz, On the definition and computation of the basic reproduction ratio R_0 in models for infectious diseases in heterogeneous populations, J. Math. Biol. 28 (1990) 503–522.
[53] P. van den Driessche, J. Watmough, Reproduction numbers and sub-threshold endemic equilibria for compartmental models of disease transmission, Math. Biosci. 180 (2002) 29–48.
[54] F. Demissie, A. Kebede, T. Shimels, P. Beyene, Assessment of public health implication of malaria-geohelminth co-infection with an emphasis on hookworm-malaria anemia among suspected malaria patients in asendabo, southwest ethiopia, Ethiop Med. J. 47 (2) (2009) 153–158.
[55] WHO, Countries and territories certified malaria-free by WHO, 2019, https://www.who.int/malaria/areas/elimination/malaria-free-countries/en/.
[56] World Health Organization, World Malaria Report 2018, 2019, https://www.who.int/malaria/media/world-malaria-report-2018/en/. Accessed: 2019.
[57] L. Facchinelli, A.R. North, C.M. Collins, M. Menichelli, T. Persampieri, A. Bucci, R. Spaccapelo, A. Crisanti, M.Q. Benedict, Large-cage assessment of a transgenic sex-ratio distortion strain on populations of an African malaria vector, Parasites Vectors 12 (2019) 70.
[58] Philip Lounibos, R.L. Escher, Sex ratios of mosquitoes from long-term census of Florida tree holes, J. Am. Mosq. Control Assoc. 24 (1) (2008) 11–15.
[59] R. Galizi, L.A. Doyle, M. Menichelli, F. Bernardini, A. Deredec, A. Burt, B.L. Stoddard, N. Windbichler, A. Crisant, A synthetic sex ratio distortion system for the control of the human malaria mosquito, Nature Commun. 5 (2014) 3977.
[60] P.W. Gething, D.C. Casey, D.J. Weiss, et al., Mapping *Plasmodium falciparum* Mortality in africa between 1990 and 2015, New Engl. J. Med. 375 (25) (2016) 2435–2445.
[61] World Health Organization. 2012. World Malaria Report 2012. Geneva, Switzerland.
[62] World Health Organization, World Malaria report 2015, 2015, http://www.who.int/malaria/publications/world-malaria-report-2015/report/en/.
[63] World Health Organization, World Malaria Report 2018, 2019, https://www.who.int/publications-detail/world-malaria-report-2019. Accessed: 2019.
[64] F.O. Okumu, S.J. Moore, Combining indoor residual spraying and insecticide-treated bednets for malaria control in Africa: a review of possible outcomes and an outline of suggestions for the future, Malar. J. 10 (2011) 208.
[65] World Health Organization, Malaria: Draft global technical strategy, in: Sixty-Eighth World Health Assembly, March 20, 2015, 2015.